

1 **Dietary emulsifiers directly impact adherent-invasive *E. coli* gene expression**
2 **to drive chronic intestinal inflammation**

3
4 Emilie Viennois^{1,2,3}, Alexis Bretin¹, Philip E. Dubé⁴, Alexander C. Maue⁴, Charlène Dauriat^{3,5}
5 Nicolas Barnich⁶, Andrew T. Gewirtz¹ and Benoit Chassaing^{1,3,5,7,8}
6

7 ¹ Institute for Biomedical Sciences, Center for Inflammation, Immunity and Infection, Digestive
8 Disease Research Group, Georgia State University, Atlanta, GA, USA

9 ² INSERM, U1149, Center of Research on Inflammation, Paris, France

10 ³ University of Paris, Paris, France.

11 ⁴ Taconic Biosciences Inc, Rensselaer, NY

12 ⁵ INSERM, U1016, team “*Mucosal microbiota in chronic inflammatory diseases*”, Paris, France.

13 ⁶ Université Clermont Auvergne/Inserm U1071; USC-INRA 2018, Microbes, Intestin,
14 Inflammation et Susceptibilité de l'Hôte (M2iSH), Clermont-Ferrand, France

15 ⁷ Neuroscience Institute, Georgia State University, Atlanta, GA

16 ⁸ Corresponding author and lead contact

17
18 **Running Title:** AIEC mediate emulsifier detrimental effects.

19
20 **Corresponding Authors:**

21 Benoit Chassaing, Ph.D.

22 INSERM, U1016, team “*Mucosal microbiota in chronic inflammatory diseases*”

23 Paris, France

24 E-Mail: benoit.chassaing@inserm.fr
25

26 **Lead Contact**

27 Benoit Chassaing, Ph.D.

28 INSERM, U1016, team “*Mucosal microbiota in chronic inflammatory diseases*”

29 Paris, France

30 E-Mail: benoit.chassaing@inserm.fr
31

32 **Abbreviations:** ASF, altered Schaedler flora; CMC, carboxymethylcellulose; IL-10, interleukin-
33 10; P80, polysorbate-80; IBD, inflammatory bowel disease.

34 **SUMMARY**

35 Dietary emulsifiers carboxymethylcellulose (CMC) and Polysorbate-80 (P80) disturb gut
36 microbiota, promoting chronic inflammation. Mice with minimal microbiota are protected
37 against emulsifiers effects, leading us to hypothesize that these compounds might provoke
38 pathobionts to promote inflammation. Gnotobiotic WT and IL10^{-/-} mice were colonized with
39 Crohn's disease-associated adherent-invasive *E. coli* (AIEC) and subsequently administered
40 CMC or P80. AIEC colonization of GF and ASF mice results in chronic intestinal inflammation
41 and metabolism dysregulations when consuming emulsifier. In IL10^{-/-} mice, AIEC mono-
42 colonization results in severe intestinal inflammation in response to emulsifiers. Exposure of
43 AIEC to emulsifiers *in vitro* increase its motility and ability to adhere to intestinal epithelial
44 cells. Transcriptomic analysis reveal that emulsifiers directly induce expression of clusters of
45 genes that mediate AIEC virulence and promotion of inflammation. To conclude, emulsifiers
46 promote virulence and encroachment of pathobionts, providing a means by which these
47 compounds may drive inflammation in hosts carrying such bacteria.

48

49 **Key Words:** Emulsifier, adherent-invasive *Escherichia coli*, intestinal inflammation, flagellin.

50 INTRODUCTION

51 Intestinal inflammation is a central feature of many of the chronic inflammatory diseases
52 that are increasingly afflicting developed, and developing, countries. For example, inflammatory
53 bowel diseases (IBD), which include Crohn's disease and ulcerative colitis, and whose central
54 defining feature is histopathologically-evident intestinal inflammation, has steadily increased
55 since the mid-20th century and now afflicts more than 20 million people worldwide (Ng et al.,
56 2017). Moreover, it is increasingly appreciated that low-grade intestinal inflammation, is
57 associated with, and promotes, a variety of other chronic disease states including colon cancer
58 and metabolic syndrome, whose features include obesity and dysglycemia (Cani et al., 2012;
59 Chassaing and Gewirtz, 2014, 2016). Determinants of chronic intestinal inflammation include
60 host genetics and gut microbiota composition, with IBD requiring a genetic predisposition to
61 disease development (Xavier and Podolsky, 2007). In contrast, metabolic syndrome and colon
62 cancer are associated with, and promoted by, microbiota dysbiosis in a wide variety of host
63 genetic backgrounds (Arthur et al., 2012; Vijay-Kumar et al., 2010). While microbiota dysbiosis
64 associated with gut inflammation is itself complex and varied, it frequently involves decreased in
65 the abundance of some phyla, together with a greater relative abundance in Enterobacteriaceae
66 (Chassaing and Darfeuille-Michaud, 2011). One specific bacteria associated with gut
67 inflammation, particularly IBD is a pathovar of *Escherichia coli* (*E. coli*) named Adherent-
68 invasive *E. coli* (AIEC) (Darfeuille-Michaud et al., 2004; Palmela et al., 2018). AIEC is
69 implicated in the pathology of Crohn's disease, especially by its ability to adhere to and invade
70 intestinal epithelial cells through expression of numerous virulence factors (Barnich et al., 2004;
71 Barnich et al., 2007; Chassaing et al., 2011b; Glasser et al., 2001; Rolhion et al., 2007).

72 Development of gut inflammation is also influenced by diet, at least in part as a result of
73 the influence of diet on gut microbiota composition (Laudisi et al., 2018; Nickerson et al., 2014;
74 Nickerson and McDonald, 2012; Rodriguez-Palacios et al., 2018; Suez et al., 2014; Tobacman,
75 2001), with various elements of macronutrient content influencing microbiota and proneness to
76 development of gut inflammation (Chassaing et al., 2015c; Llewellyn et al., 2018; Miles et al.,
77 2017). Additionally, some food additives can promote gut inflammation. For example, and
78 centrally relevant to this study, carboxymethylcellulose (CMC) and Polysorbate 80 (P80), which
79 are commonly used synthetic emulsifiers that are added to a variety of processed foods to
80 enhance texture and extend shelf-life, alter microbiota in a manner that promotes intestinal
81 inflammation. More specifically, we have shown that administration of CMC or P80 to mice
82 resulted in microbiota encroachment into the mucus, alterations in microbiota composition,
83 including an increase of bacteria that produced pro-inflammatory flagellin and LPS, and
84 development of chronic inflammation (Chassaing et al., 2015b; Chassaing et al., 2017b; Viennois
85 and Chassaing, 2018). Such inflammation was associated with low-grade inflammation and
86 metabolic syndrome in WT mice and increased incidence/severity of colitis in genetically
87 susceptible mice (interleukin-10 (IL-10)^{-/-}) (Chassaing et al., 2015b). Furthermore, emulsifier
88 consumption increased the susceptibility of mice to developing colonic tumors by creating and
89 maintaining a proinflammatory environment associated with an altered proliferation/apoptosis
90 balance (Viennois et al., 2017). While precise determination of emulsifier exposure in humans is
91 challenging, average consumption of CMC and P80 are 46 and 8.2 mg/kg/bw/day in the United
92 Kingdom, respectively (Cox et al., 2020; EFSA, 2015, 2017). Although average intakes in
93 humans appear lower than doses we previously used in mouse models, our animal studies
94 employed relatively short-term emulsifier exposure (Chassaing et al., 2015b; Chassaing et al.,

95 2017b) and the chronic nature of human intake over many years might allow to reach similar
96 exposure levels. Moreover, we previously investigated the impact of these compounds
97 individually, while processed food often simultaneously contain multiple dietary emulsifiers
98 with, likely, additive or synergistic effects (Chassaing et al., 2015b; Chassaing et al., 2017b; Cox
99 et al., 2020). While results from clinical trials on emulsifiers are not yet available, the
100 observations that diets lacking emulsifiers and other suspected triggers of IBD are more effective
101 than elemental diet in maintaining remission of pediatric CD highlights the importance of dietary
102 triggers in IBD (Levine et al., 2019; Sabino et al., 2019).

103 That CMC and P80 did not induce low-grade gut inflammation or indices of metabolic
104 syndrome in germ-free mice highlights that these compounds perturb host-microbiota
105 homeostasis rather than directly trigger host pro-inflammatory gene expression (Chassaing et al.,
106 2015b; Chassaing et al., 2017b; Viennois et al., 2017). Moreover, these compounds did not
107 discernably impact mice harboring only a limited defined pathobiont-free microbiota, namely
108 Altered Schaedler Flora (ASF) (Chassaing et al., 2017b), leading us to hypothesize that
109 emulsifiers may not uniformly impact bacteria per se but rather provoke responses from
110 pathobiont bacteria, particularly those, such as AIEC, that can induce virulence gene expression
111 in response to select environmental conditions. Herein, we tested this hypothesis by
112 administering CMC or P80 to gnotobiotic mice colonized by AIEC and, moreover, by directly
113 examining the impact of these compounds on AIEC gene expression *in vitro*. We found that
114 presence of AIEC was sufficient to make mice prone to the detrimental impacts of CMC and
115 P80. Moreover, exposure to these compounds directly promoted AIEC virulence, as assessed by
116 non-targeted transcriptomic analysis and ability to adhere to gut epithelial cells. These results

117 suggest that CMC and P80 might promote ability of pathobionts to colonize the intestine and
118 promote gut inflammation and its associated disease states.

119 **RESULTS**

120 *AIEC confers proneness to detrimental effects of dietary emulsifiers*

121 Administration of the dietary emulsifiers CMC and P80 to WT mice results in low-grade
122 intestinal inflammation and metabolic syndrome (Chassaing et al., 2015b; Chassaing et al.,
123 2017b). Such emulsifier-induced phenotypes were absent in germ-free mice as well as in ASF
124 mice, which are colonized with a low complexity microbiota (Chassaing et al., 2017b), leading
125 us to hypothesize that emulsifiers might promote gut inflammation by acting upon pathobiont
126 bacteria that are present in many hosts. Hence, we investigated if addition of AIEC to ASF mice
127 would render them prone to pro-inflammatory impacts of CMC and P80. ASF mice were
128 colonized with AIEC reference strain LF82 (Darfeuille-Michaud et al., 2004), as outlined in
129 **Figure S1A**, and the impact of emulsifier on intestinal inflammation and metabolism measured.
130 ASF/AIEC mice administered either CMC or P80 displayed a range of features of intestinal
131 inflammation, including increased colon weight, colon shortening, increases in colon
132 weight/length ratio, as well as a non significant tendency toward increased spleen weight and
133 elevated levels of fecal lipocalin-2 (Lcn2) (**Figure 1A-G**). Such indices of inflammation were
134 associated with increased intestinal expression of genes that promote and/or reflect inflammation
135 (**Figure 1H-I and S1C-F**). Moreover, histological scoring of colonic sections indicated a
136 significantly increased inflammation in CMC- and P80-treated mice compared with control
137 animals (**Figure 1J and S1K**). Furthermore, such emulsifier-induced intestinal inflammation
138 was associated with features of metabolic syndrome including elevations in body weight, fat pad
139 mass, and fasting levels of blood glucose (**Figure 1 K-M**). Combination of all these
140 morphological and molecular measurements of inflammation into principal coordinate analysis
141 using Bray-Cruttis distance showed a clear and significant clustering of CMC- and P80-treated

142 animals compared with control animals, further highlighting the increase in inflammation level in
143 emulsifier treated mice (**Figure S1G**). Together, these data indicate that, like conventional mice,
144 and in contrast to ASF mice, which are fully protected against emulsifier-induced intestinal
145 inflammation and metabolic deregulation (Chassaing et al., 2017b), mice colonized by AIEC
146 amidst the ASF community are susceptible to emulsifier-induced low-grade inflammation and its
147 metabolic consequences.

148

149 *AIEC colonization results in alterations in microbiota composition upon emulsifier treatment*

150 We envisaged that emulsifiers might have led to inflammation in ASF/AIEC mice *via*
151 promoting increased AIEC abundance and/or more general alteration in microbiota composition
152 and/or activity. To investigate these possibilities, we first examined the impact of emulsifiers on
153 gut microbiota composition of AIEC/ASF mice *via* 16S rRNA gene sequencing. While we
154 previously reported that ASF mice are fully protected against emulsifiers-induced alterations in
155 microbiota composition (Chassaing et al., 2017b), principal coordinate analysis of the
156 unweighted Unifrac distance revealed clear alteration in the microbiota composition of P80-
157 treated AIEC/ASF mice at day 56 compared to their water-treated counterpart (**Figure 2A-C**,
158 Permanova p-value=0.015). This alteration in microbiota composition was not driven by an
159 alteration in the relative abundance of AIEC (**Figure 2D**, based on 16S data), but rather by
160 changes in levels of ASF species with, for example, a complete loss of the Clostridiaceae family
161 (ASF 356 and/or ASF 502 (Gomes-Neto et al., 2017)) in P80-treated mice (**Figure S2A**). In
162 contrast, CMC administration did not result in a clear overall difference in microbiota of
163 AIEC/ASF mice but was associated with subtle alterations such as an increase in members of the
164 Clostridiaceae family (**Figure S2A**, ASF 356 and/or ASF 502 (Gomes-Neto et al., 2017)) and a

165 tendency toward a decrease in *Parabacteroides* genus (**Figure S2B**, ASF 519 (Gomes-Neto et
166 al., 2017)). These results are in accord with our previous studies using an *in vitro* microbiota
167 system that suggested that P80 directly alters microbiota composition while CMC directly
168 impacts microbiota gene expression (Chassaing et al., 2017b).

169

170 We next examined the extent to which CMC and P80 functionally impacted ability of
171 microbiota to promote intestinal inflammation. One important mediator of host-bacterial
172 interactions is bacterial flagella, which confers motility and whose major component flagellin
173 directly activates host pro-inflammatory gene expression *via* TLR5 and NLRC4 (Franchi et al.,
174 2006; Hayashi et al., 2001). Hence, we used TLR5 reporter cells and observed that, in contrast to
175 ASF mice that do not show any alteration in fecal flagellin in presence of emulsifiers (Chassaing
176 et al., 2017b), CMC or P80 consumption by ASF mice colonized by AIEC resulted in higher
177 levels of flagellin (**Figure 2E-F**), while fecal lipopolysaccharide levels were not affected by
178 emulsifier consumption (**Figure 2G-H**). Use of quantitative PCR applied to purified fecal DNA
179 demonstrated that this increase in fecal flagellin was not due to alteration in fecal bacterial
180 density nor fecal AIEC abundance (**Figure 2I-J**). One potential consequence of increased
181 flagella is a greater ability to penetrate the mucus layer resulting in decreased bacterial-epithelial
182 distance (i.e. microbiota encroachment), which is a feature of gut inflammation in IBD and
183 metabolic syndrome (Chassaing et al., 2015b; Chassaing et al., 2014b; Chassaing et al., 2017a;
184 Sevrin et al., 2018). Confocal analysis of Carnoy-fixed colon specimen to measure the distance
185 separating intestinal bacteria from the surface of the epithelium revealed microbiota
186 encroachment in ASF/AIEC mice that had consumed CMC or P80 (**Figure 3A-D**). In light of
187 these results, we measured intestinal expression of mucin-2 as well as lectin-like protein ZG16

188 (zymogen granulae protein 16), an abundant mucus protein that contributes to maintenance of
189 bacteria-epithelial distance (Bergstrom JH, 2016, PNAS) and Ly6/PLAUR domain containing 8
190 (Lypd8), which prevents flagellated microbiota to invade the colonic epithelia. We found that
191 expression of both ZG16 and Lypd8 was increased in CMC-treated ASF/AIEC mice compared
192 to control mice (**Figure S1I-J**), while expression of mucin-2 was unchanged (**Figure S1H**).
193 These results suggest that the host responses to repel encroaching bacteria remain functional and
194 are consistent with the notion that promotion of encroachment by emulsifiers might reflect
195 impacts on microbiota. To further understand how CMC and P80 impacted microbiota-epithelial
196 interactions, we utilized laser capture microdissection, which we recently developed as a means
197 to identify inner mucus microbiota (Chassaing and Gewirtz, 2019). This approach indicated that
198 in ASF/AIEC mice, irrespective of emulsifier treatment, a striking majority of the inner mucus
199 bacteria were proteobacteria, specifically AIEC strain LF82 since the ASF community originally
200 lacks Proteobacteria (63.2-82.9%, **Figure 3E**). While neither CMC or P80 markedly impacted
201 relative microbiota composition of inner mucus (**Figure S2C**), the high abundance of AIEC
202 close to the epithelium suggests impacts of emulsifiers on this bacterium might play a key role in
203 mediating impacts of these compounds on the intestine.

204

205 *AIEC, by itself, is sufficient to make mice prone to detrimental effects of emulsifiers*

206 To investigate the extent to which the impact of CMC and P80 on ASF/AIEC was
207 mediated by AIEC alone or reflected that AIEC can have a long lasting impact on microbiota
208 composition (Bretin et al., 2018; Chassaing et al., 2014a), we mono-colonized germ-free mice
209 with the AIEC reference strain LF82 and subsequently subjected these mice to emulsifier
210 treatment. As presented in **Figure 4**, AIEC by itself made mice prone to pro-inflammatory

211 impacts of CMC and P80, as reflected by colon weight, colon length and slight increase in spleen
212 weight (**Figure 4A-G**). Moreover, histological scoring of colon specimens indicated significantly
213 increased inflammation in CMC- and P80-treated animals compared to control mice (**Figure 4H**
214 **and S2D**). Such indices of low-grade inflammation correlated with mild increases in adiposity,
215 although impacts on overall weight was not observed (**Figure 4I-J**). Analogous to observation in
216 ASF mice, combination of all these morphological and molecular measurements into principal
217 coordinate analysis using the Bray-Curtis distance demonstrated a clear and significant clustering
218 of CMC- and P80-treated animals compared with control AIEC monocolonized animals (**Figure**
219 **S2E**).

220 We next investigated the intestinal behavior of AIEC LF82 bacteria in response to CMC
221 and P80 exposure. Use of quantitative PCR to quantitate fecal levels of AIEC indicated that
222 absolute AIEC abundance was not impacted by CMC or P80 (**Figure 4K**). However, confocal
223 analysis of Carnoy-fixed colon specimen to measure the distance separating AIEC LF82 bacteria
224 from the surface of the epithelium revealed bacterial encroachment in AIEC mono-colonized
225 mice that had consumed CMC or P80 (**Figure 4L**), suggesting that emulsifier-induced alterations
226 in AIEC gene expression promoted an encroaching phenotype. In any case, collectively, these
227 results indicate that AIEC is sufficient to make mice prone to detrimental impacts of CMC and
228 P80, with the observation that such effects are more pronounced when additional microbial
229 species, such as ASF members, are present.

230

231 We next examined if AIEC, by itself, would confer proneness to developing colitis upon
232 emulsifier treatment in IL10^{-/-}, which are highly susceptible to developing this disorder in
233 conventional condition but not under germ-free condition (Kuhn et al., 1993; Sellon et al., 1998).

234 Germ-free IL10^{-/-} mice were mono-colonized with AIEC reference strain LF82 and subsequently
235 administered CMC or P80. Most (80%) of the AIEC-colonized IL-10^{-/-} mice died within 40 days
236 of P80 treatment with marked signs of gut inflammation including slight increase in spleen
237 weight and colon shortening (**Figure 5A-F**). Such severe illness was not seen in CMC-treated
238 mice, rather, such mice displayed evidence of mild inflammation including colon shortening
239 amidst an increased colon weight (**Figure 5A-F**), further illustrating the different impact of CMC
240 and P80 on the host-microbiota relationship, as previously reported (Chassaing et al., 2017b).
241 Analysis of colon expression of CXCL-1, IL1- β , TNF- α by q-RT-PCR supported the notion that
242 AIEC-monoassociated IL10^{-/-} mice were prone to emulsifier-induced gut inflammation (**Figure**
243 **5G-I**), while expression of IL-6 and IL-22 was unchanged (**Figure S3A-B**). Combinatorily
244 assessing these morphological and molecular measurements *via* principal coordinate analysis of
245 Bray-Crutis distance revealed a clear and significant clustering of CMC- and P80-treated animals
246 compared with control AIEC monocolonized IL10^{-/-} mice (**Figure S3C**). In accord with previous
247 work reporting that high levels of TNF α and IL-1 β promote cachexia, gut inflammation in IL-10^{-/-}
248 mice did not result in metabolic syndrome (**Figure 5J-K**).

249

250 Another consequence of the inflammation promoted by CMC and P80 is increased
251 proneness to colitis-associated cancer, which was modeled by an AOM injection and repeated
252 exposures to DSS (Viennois et al., 2017). Hence, we examined if mice mono-colonized with
253 AIEC LF82 and concomitantly treated with emulsifiers would exhibit increased carcinogenesis
254 upon AOM/DSS treatment, as schematized in **Figure S1B**. As presented **figure 5L-M**, CMC
255 consumption, but not P80, significantly increased the total tumor count and total tumor area in
256 AIEC mono-colonized mice and enhanced associated intestinal inflammation (**Figure S3D-I**).

257 Such increased tumor burden suggested the possibility of increased cell proliferation in CMC-
258 treated mice. In accord with this possibility, analysis of proliferation of colonic epithelial cells by
259 Ki67 staining revealed that the consumption of emulsifier by itself (i.e., no AOM/DSS) increased
260 cell proliferation compared with AIEC-mono-colonized water-treated control group (**Figure S4**).
261 AOM/DSS treatment increased the number of Ki67-positive cells in all groups of mice, but the
262 proliferation level remained significantly higher in AOM/DSS-treated mice that had consumed
263 CMC, in accordance with the increased tumor burden observed in this group (**Figure S4**), while
264 P80 exposure did not impacted epithelial cells proliferation. To further address the role of cell
265 turnover in AIEC/emulsifier promotion of colonic carcinogenesis, TUNEL-based quantification
266 of apoptosis in colonic sections was performed. Analogous to our results for cell proliferation,
267 we observed that consumption of emulsifiers by itself (i.e., no AOM/DSS) increased the basal
268 level of TUNEL+ cells in AIEC mono-colonized mice (**Figure S5**). Moreover, this difference
269 between water- and emulsifier-consuming groups was further increased in response to
270 AOM/DSS treatment (**Figure S5**), indicating that AIEC/emulsifier combination is sufficient to
271 upregulates both apoptosis/proliferation in the intestinal epithelium, resulting in increased cell
272 turnover that can promote tumorigenesis.

273 Altogether, these data suggest that AIEC bacteria are sufficient to confer proneness to
274 emulsifier-induced intestinal inflammation in WT and genetically susceptible hosts. Such
275 inflammation is sufficient to promote detrimental phenotypes of such inflammation, which are
276 influenced by host genetics and numerous other environmental factors. Moreover, the various
277 models used above further exemplify that CMC and P80 alter the host/microbiota homeostasis
278 through both shared and unique mechanisms.

279

280
281
282
283
284
285
286
287
288
289
290
291
292
293
294
295
296
297
298
299
300
301
302

Dietary emulsifiers increase adherent-invasive Escherichia coli pathogenic potential through transcriptome modulation

The results described above suggests that understanding direct impacts of emulsifiers on AIEC might elucidate mechanisms underlying detrimental impacts of these compounds. Hence, we examined impacts of CMC and P80 on AIEC *in vitro*. We first investigated the impact of emulsifier exposure on the defining features of AIEC, namely ability to adhere to and invade intestinal epithelial cells. Only subtle inhibitory effects on AIEC growth *in vitro* were observed for both CMC and P80 (**Figure S6A-B**), which aligns with our *in vivo* observations that fecal AIEC density is not impacted by emulsifiers exposure. However, we observed that both CMC and P80 increased AIEC adhesion to Int-407 intestinal epithelial cells in a dose dependent manner (**Figure 6A**), while invasion ability was not affected (**Figure 6B**). We next broadly examined the impact of CMC and P80 on AIEC gene expression *via* RNA-Seq approach. CMC dramatically impacted the AIEC LF82 transcriptome in a concentration-dependent manner, as shown in the volcano plots **Figure 6C**. CMC impacted expression of both chromosomal and plasmid gene expression (**Figure S6C-D**). In contrast, this approach indicated that P80 had only a modest impact on AIEC gene expression. Use of Principal coordinate analysis to visualize these transcriptomes confirmed that CMC induced a strong concentration-dependent alteration in the AIEC transcriptome, while P80 had a subtler, albeit significant, effect (**Figure S7A-B**). Bacterial genes impacted by emulsifier exposure included virulence factors and genes involved in numerous processes, including LPS biosynthesis, DNA replication and transcription (**Figure S7C-G**). For example, expression of *diaA*, which encodes a DnaA initiator-associating protein,

303 was significantly induced by both CMC and P80 in a dose dependent manner (**Figure S7F**),
304 indicating a broad impact of emulsifier on AIEC replication and fitness (Keyamura et al., 2007).
305 Among numerous virulence factors expressed by AIEC bacteria, flagella (composed by the
306 major sub-unit flagellin FliC and regulated by the FlhDC master regulator), type 1 pili
307 (composed by the major sub-unit FimA) and long polar fimbriae (composed by the major sub-
308 unit LpfA) are known to play central role in bacterial motility, adhesion, and Peyer's patches
309 targeting, respectively (for review, (Palmela et al., 2018)). Expression of these virulence factors
310 was significantly increased by CMC in a dose dependent manner (**Figure 6D**), while the effect of
311 P80 seems minimal in regulating AIEC virulence gene expression. Additionally, other genes
312 encoding known AIEC virulence factors were also significantly impacted by emulsifier
313 exposure, as presented in the heatmap **figure S7C**, where CMC induced the expression of
314 numerous known AIEC virulence factors, while P80 had an effect on type VI secretion system.
315 Hence, CMC, and to a much lesser extent, P80, can be directly sensed by AIEC bacteria, leading
316 to alteration in bacterial transcriptome and increases in the expression of numerous virulence
317 factors.

318

319 *Flagella contributes to AIEC's mediation of emulsifier-induced inflammation*

320 In accord with its impacts on AIEC gene expression, CMC significantly increased
321 flagella-mediated AIEC motility (**Figure 6E**), while P80 did not impact such phenotype. In light
322 of the potential role of flagella/motility in mediating AIEC's promotion of inflammation and
323 mucus penetration (Carvalho et al., 2012; Chassaing et al., 2014a; Sevrin et al., 2018), we next
324 examined if flagellin was necessary for AIEC to confer proneness to emulsifier-induced
325 inflammation. Germ-free WT mice were mono-colonized with AIEC LF82- Δ fliC isogenic

326 mutant and subsequently subjected to emulsifier treatment. Mice monoassociated with aflagellate
327 AIEC exhibited only modest evidence of intestinal inflammation in response to CMC, which was
328 not associated with indices of metabolic syndrome, while P80 wholly lacked impacts in such
329 mice (**Figure 7 and S8**). Moreover, in these LF82- Δ *fliC* mono-colonized mice, the proliferative
330 status of the epithelium was normalized in P80-treated group while the apoptosis activity was
331 normalized in both CMC- and P80-treated group, suggesting a key role played by AIEC flagella
332 in altering the intestinal epithelial cell turnover following emulsifier consumption (**Figure S4**
333 **and S5**). Hence, the ability of emulsifiers to increase AIEC's promotion of intestinal
334 inflammation appear to be mediated, in part, by flagella.

335 **DISCUSSION**

336 The intestinal microbiota plays a critical role in mediating the impacts of diet
337 composition upon health (Zmora et al., 2019). The best understood example of this notion is the
338 catabolism of complex carbohydrates by gut bacteria into short-chain fatty acids, which aids
339 energy harvest and has a variety of beneficial impacts upon intestinal health. Moreover, the
340 ability of microbiota composition to broadly predict post-prandial glycemic control in response
341 to a variety of foods underscores the role of specific bacterial taxa in mediating how diet impacts
342 the host (Zeevi et al., 2015). Microbiota is also a key mediator of some of the detrimental
343 impacts that some diets can have on their host. The example germane to this present study is our
344 observation that mice administered 2 common synthetic dietary emulsifiers, CMC and P80,
345 develop gut inflammation that can promote a range of disease states including colitis, metabolic
346 syndrome, and cancer (Chassaing et al., 2015b; Viennois et al., 2017). Such emulsifier-induced
347 inflammation is mediated by microbiota in the sense that it correlates with changes in microbiota
348 composition and localization, and that emulsifiers lack discernable impacts in germ-free mice.
349 Emulsifiers also lack impact in ASF mice, which have a very limited microbiota (Chassaing et
350 al., 2017b), thus suggesting that CMC and P80 disturb the complex inter-relationship between
351 the intestine and the diverse microbial ecosystem it normally harbors, while how such
352 disturbance occur remained unclear. Our findings herein that emulsifiers can directly elicit
353 virulence gene expression and encroachment within the inner mucus inner by pathobiont *E. coli*
354 in a way that is sufficient to make mice prone to detrimental impacts of these compounds help
355 fill this gap of knowledge.

356 The observation that, in contrast to ASF mice, mice carrying only AIEC or carrying
357 AIEC amidst the other ASF species display emulsifier-induced inflammation leads us to

358 conclude that the presence of AIEC is sufficient to mediate the detrimental impacts of CMC and
359 P80. While it is more difficult to make firm conclusions regarding how the presence of AIEC
360 makes mice prone to emulsifiers, the ability of these compounds to directly elicit AIEC virulence
361 gene expression *in vitro* suggests a plausible mechanism. Specifically, we hypothesize that, *in*
362 *vivo*, consumption of CMC and P80, which are non-absorbed, results in their direct interaction
363 with AIEC, increasing expression of genes that facilitate its penetration of the mucus layer and
364 adherence to epithelial cells, resulting in activation of host pro-inflammatory signaling. Hence,
365 we propose that carriage of AIEC may be one specific determinant of the extent to which an
366 individual will be prone to inflammation upon consumption of emulsifiers.

367

368 Studies of basic microbial pathogenesis in classic pathogens such as *Salmonella* and
369 Enterohemorrhagic *E. coli* have revealed complex mechanisms of sensing the environment
370 allowing robust and rapid induction virulence gene expression under select conditions (Duprey et
371 al., 2014; Fang et al., 2016; Jubelin et al., 2018). That AIEC is known to have somewhat
372 analogous sensing machinery (Chassaing and Darfeuille-Michaud, 2013; Chassaing et al., 2013;
373 Chassaing et al., 2011a; Rolhion et al., 2007; Sevrin et al., 2018; Vazelle et al., 2016) suggests
374 that emulsifiers might impact bacterial surfaces due to their detergent properties. Specifically, it
375 suggests the possibility that these compounds may alter AIEC permeability to select molecules,
376 thus altering AIEC periplasm homeostasis, known to play a central role in the regulation of
377 virulence gene expression by AIEC bacteria (Chassaing and Darfeuille-Michaud, 2013;
378 Chassaing et al., 2015a; Rolhion et al., 2007). Such a mechanism offers a potential explanation
379 as to why CMC and P80 might have somewhat similar but yet also distinct impacts on AIEC
380 gene expression, in that these chemically distinct detergents would likely impact permeability in

381 unique ways. Such a mechanism could also potentially explain the seemingly unusual
382 concentration-dependent effect of P80, in that a low concentration of P80 might permit impact
383 AIEC permeability to specific molecules while higher concentration may also increase
384 permeability to other molecules with countering effect. In any event, analogous dose-dependence
385 of P80 was previously observed *in vivo* (Chassaing et al., 2015b; Chassaing et al., 2017b).

386

387 That CMC had a stronger impact on AIEC virulence gene expression than P80 mimics
388 our work with complex human microbiotas in the simulated human intestinal microbiota
389 ecosystem (SHIME) model, in which CMC had a rapid pronounced impact on microbial gene
390 expression that did not associate with differences in species composition (Chassaing et al.,
391 2017b). Conversely, that P80 altered microbiota composition in the SHIME system mimics our
392 observations herein that, in AIEC/ASF mice, only P80 markedly impacted microbiota
393 composition. While the mechanisms explaining these differential impacts of CMC and P80 are
394 not known, they are also potentially explainable by direct impacts of these compounds on
395 microbial surfaces. Interestingly, the detergent-like properties of emulsifiers were pivotal in
396 leading Rhodes and colleagues, and subsequently ourselves, to hypothesize that these
397 compounds might impact host-microbiota interactions and subsequently gut inflammation
398 (Chassaing et al., 2015b; Roberts et al., 2010; Roberts et al., 2013). However, this hypothesis
399 was based on the notion that emulsifiers might impact the functional properties of mucus. While
400 this possibility remains under consideration, our attempts to generate data in support of it have
401 not yet been successful. Rather, our results to date suggest that the impact of emulsifiers on
402 bacteria themselves are sufficient to explain their detrimental impacts.

403

404 Direct impacts of emulsifiers on AIEC results in changes in expression of hundreds of
405 genes, in which many of the upregulated genes are putative virulence factors. While we presume
406 that many of these might have potentially important roles in promoting inflammation, that an
407 AIEC flagellar mutant conferred only slight proneness to emulsifier-induced inflammation
408 supports a central role for flagella in mediating impacts of these compounds. Such a role may
409 reflect a role for flagella in mediating mucus penetration, adherence, or activation of innate
410 immune signaling *via* TLR5 or the NLRC4 inflammasome. Future experimentation will be
411 needed to distinguish these possibilities and determine the relative importance of numerous other
412 genes induced by emulsifiers.

413 **CONCLUSION**

414 We demonstrated here that dietary emulsifier upregulate AIEC virulence gene
415 expression, promoting intestinal inflammation. Moreover, this study further highlights
416 specificities of CMC and P80 effects on pathobionts, suggesting a synergistic detrimental effects
417 of emulsifiers when present in combinations, as it is often the case in processed foods. While
418 determining the importance of emulsifier impacts upon AIEC amidst a complex microbiota
419 remains an important challenge for future studies, we presume that multiple emulsifier-
420 responsive bacteria might be present. Hence, we submit that the extent to which non-absorbed
421 food additives can act directly upon select microbial taxa may prove to be an important
422 consideration in predicting detrimental impacts of food additives (Viennois et al., 2019).
423 Moreover, these findings further support the need for microbiota-based dietary intervention in
424 the management of chronic gut inflammation, in which individuals carrying specific microbiota
425 members will benefit from targeted dietary recommendations.

426 **ACKNOWLEDGEMENTS**

427 This work was supported by an Innovator Award from the Kenneth Rainin Foundation.
428 Moreover, E.V. is a recipient of the Career Development Award from the CCF and an Individual
429 Fellowship Marie Sklodowska-Curie grant from the European Commission Research Executive
430 Agency. B.C. is supported by a Starting Grant from the European Research Council, a Chaire
431 d'Excellence from Paris University and a Career Development Award from the Crohn's and
432 Colitis Foundation (CCF). A.T.G. is supported by NIH grant DK099071 and DK083890.
433 Funders had no role in the design of the study and data collection, analysis and interpretation, nor
434 in manuscript writing. We thank the Hist'IM and Imag'IC platforms (INSERM U1016, Paris,
435 France) for their help.

436

437 *This work is dedicated to the memory of Arlette Darfeuille-Michaud who pioneered the*
438 *identification and characterization of AIEC bacteria. In loving memory.*

439

440 **AUTHOR CONTRIBUTIONS**

441 BC obtained funding and conceived and supervised the study. EV, AB, CD and BC
442 performed lab work, analyzed the data, performed statistical analyses, and wrote the manuscript.
443 EV, PED, ACM, NB, ATG and BC analyzed the data and wrote the manuscript. All authors
444 approved the final version of the manuscript.

445

446 **DECLARATION ON INTEREST**

447 The authors declare that they have no competing interests.

448 **FIGURE LEGENDS**

449 **Figure 1: Colonization by adherent-invasive *Escherichia coli* bacteria is sufficient to**
450 **promote detrimental effects of emulsifiers in normally protected ASF mice.** Six-week-old
451 ASF C57BL/6 mice were colonized with AIEC reference strain LF82 and subsequently exposed
452 to CMC or P80 diluted in drinking water (1.0%) for 12 weeks. (A) Colon weight, (B) colon
453 length, (C) colon weight / length ratio, (D) spleen weight, (E-G) fecal Lcn2 at day 0 (E), day 28
454 (F) and day 56 (G). Colonic mRNA levels of IL1- β (H) and IL10 (I). (J) colonic histological
455 score, (K) final body weight, (L) fat pad weight and (M) 5hr fasting blood glucose
456 concentration. Data are the means +/- S.E.M ($N=4-5$). * $P < .05$ compared to water-treated group,
457 determined by a one-way analysis of variance corrected for multiple comparisons with a
458 Bonferroni post-test.

459

460 **Figure 2: Colonization of ASF mice by adherent-invasive *Escherichia coli* bacteria is**
461 **sufficient to induce emulsifier-mediated alterations in microbiota.** Six-week-old ASF
462 C57BL/6 mice were colonized with AIEC reference strain LF82 and subsequently exposed to
463 CMC or P80 diluted in drinking water (1.0%) for 12 weeks. Fecal DNA was extracted and
464 microbiota composition analyzed by 16S rRNA gene sequencing. (A-C) Principal coordinate
465 analysis of the unweighted Unifrac distance at day 0 (A), day 28 (B) and day 56 (C). (D)
466 Relative abundance of the Enterobacteriaceae family in the fecal microbiota. (E-F) Fecal FliC
467 levels at day 0 (E) and day 56 (F). (G-H) Fecal LPS levels at day 0 (G) and day 56 (H). (I-J)
468 Fecal bacterial density (I) and relative abundance of AIEC LF82 bacteria at day 56 (J). Data are
469 the means +/- S.E.M ($N=4-5$). For clustering analyzing on principal coordinate plots, categories
470 were compared and statistical significance of clustering were determined using Permanova

471 method. *P < .05 compared to water-treated group, determined by a one-way analysis of
472 variance corrected for multiple comparisons with a Bonferroni post-test.

473

474 **Figure 3: Colonization by adherent-invasive *Escherichia coli* bacteria is sufficient to induce**
475 **microbiota encroachment in normally protected ASF mice.** Six-week-old ASF C57BL/6
476 mice were colonized with AIEC reference strain LF82 and subsequently exposed to CMC or P80
477 diluted in drinking water (1.0%) for 12 weeks. (A-C) Confocal microscopy analysis of
478 microbiota localization: Muc2 (green), actin (purple), bacteria (red) and DNA (blue) of water-
479 (A), CMC- (B) and P80- (C) treated mice. Bar = 20 μ m. (D) Distances of the closest bacteria to
480 intestinal epithelial cells (IEC) per condition over three high-powered fields per mouse. (E)
481 Laser capture micro-dissection of inner mucus layer was performed in order to collect mucus-
482 associated microbiota. Fecal and mucus-associated microbiota composition was analyzed by 16S
483 rRNA gene Illumina sequencing. Taxa summarization performed at the phylum level is
484 represented. Data are the means +/- S.E.M (N=4-5). *P < .05 compared to water-treated group,
485 determined by a one-way analysis of variance corrected for multiple comparisons with a
486 Bonferroni post-test.

487

488 **Figure 4: Mono-colonization by adherent-invasive *Escherichia coli* bacteria is sufficient to**
489 **drive detrimental effects of emulsifiers in WT mice.** Six-week-old germ-free C57BL/6 mice
490 were mono-colonized with AIEC reference strain LF82 and subsequently exposed to CMC or
491 P80 diluted in drinking water (1.0%) for 12 weeks. (A) Colon weight, (B) colon length, (C)
492 colon weight / length ratio, (D) spleen weight, (E-G) fecal Lcn2 at day 0 (E), day 28 (F) and day
493 56 (G), (H) colonic histological score, (I) final body weight, (J) fat pad weight, (K) relative

494 abundance of AIEC LF82 bacteria at day 56 and (L) distances of the closest AIEC bacteria to
495 intestinal epithelial cells (IEC) per condition over three high-powered fields per mouse. Data are
496 the means +/- S.E.M (N=4-5). *P < .05 compared to water-treated group, determined by a one-
497 way analysis of variance corrected for multiple comparisons with a Bonferroni post-test.

498

499 **Figure 5: Mono-colonization by adherent-invasive *Escherichia coli* bacteria is sufficient to**
500 **drive detrimental effects of emulsifiers in IL10^{-/-} mice and promotion of colon cancer in WT**
501 **mice. (A-K)** Six-week-old germ-free (GF) IL10^{-/-} C57BL/6 mice were colonized with AIEC
502 reference strain LF82 and subsequently exposed to CMC or P80 diluted in drinking water (1.0%)
503 for 12 weeks. (A) Survival curve, (B) colon weight, (C) colon length, (D) colon weight / length
504 ratio, (E) spleen weight, (F) caecum weight, (G) final body weight and (H) fat pad weight. (I-K)
505 Colonic mRNA levels of Cxcl1 (I), IL1-β (J) and TNF-α (K). (L-M) Six-week-old germ-free
506 C57BL/6 mice were mono-colonized with AIEC reference strain LF82 and subsequently
507 exposed to CMC or P80 diluted in drinking water (1.0%) for 12 weeks in combination with an
508 AOM/DSS protocol. (L) Number of tumors per mouse and (M) total surface or tumor area in
509 mm². Data are the means +/- S.E.M (N=5). *P < .05 compared to water-treated group,
510 determined by a one-way analysis of variance corrected for multiple comparisons with a
511 Bonferroni post-test.

512

513 **Figure 6: Dietary emulsifiers increase adherent-invasive *Escherichia coli* pathogenic**
514 **potential through transcriptome modulation.** Adhesion (A) and invasion (B) abilities of AIEC
515 LF82 grown *in vitro* with various concentration of CMC and P80 with intestinal epithelial cells
516 (I-407). (C) AIEC reference strain LF82 was grown *in vitro* with various concentration of CMC

517 and P80, mRNAs extracted and subjected to RNA-Seq analysis. Chromosomic genes were
518 visualized on a volcano plot as follow: Up/left: water-treated versus CMC- 1.0000%-treated;
519 up/middle: water-treated versus CMC- 0.2500%-treated; up/right: water-treated versus CMC-
520 0.0625%-treated; bottom/left: water-treated versus P80- 1.0000%-treated; bottom /middle: water-
521 treated versus P80- 0.2500%-treated; bottom /right: water-treated versus P80- 0.0625%-treated.
522 For each chromosomic gene, the difference in abundance between the two groups is indicated in
523 log₂ fold change on *x*-axis (with positive values corresponding to an increase in emulsifier-
524 treated group compare to water-treated group, and negative values corresponding to a decrease in
525 emulsifier-treated group compare to water-treated group), and significance between the two
526 groups is indicated by -log₁₀ *p*-value on the *y*-axis. Red dots correspond to chromosomic genes
527 with a *p*-value <0.05 between emulsifier-treated and water-treated groups. Orange dots
528 correspond to chromosomic genes with at least a 2-fold decreased or increased abundance in
529 emulsifier-treated group compare to water-treated group. Green dots correspond to chromosomic
530 genes with at least a 2-fold decreased or increased abundance in emulsifier-treated group
531 compare to water-treated group and with a *p*-value <0.05. **(D)** AIEC reference strain LF82 was
532 grown *in vitro* with various concentration of CMC and P80, mRNAs extracted and subjected to
533 q-RT-PCR analysis of *fliC*, *flhDC*, *fimA* and *lpfA* gene expression. **(E)** Motility assay of AIEC
534 reference strain LF82 grown *in vitro* with various CMC or P80 (1%). Bacteria were washed
535 before inoculation of 0.3% agar medium and motility was assessed quantitatively 15 hours post
536 inoculation by examining the circular swimming motion formed by the growing motile bacterial
537 cells. Data are the means +/- S.E.M (*N*=2-6). **P* < .05 compared to water-treated group,
538 determined by a one-way analysis of variance corrected for multiple comparisons with a
539 Bonferroni post-test.

540

541 **Figure 7: Bacterial flagellin contributes to AIEC-mediated emulsifier detrimental effects.**

542 Six-week-old germ-free C57BL/6 mice were mono-colonized with AIEC LF82- Δ *fliC* mutant and

543 subsequently exposed to CMC or P80 diluted in drinking water (1.0%) for 12 weeks. (A) Colon

544 weight, (B) colon length, (C) colon weight / length ratio, (D) spleen weight, (E-G) fecal Lcn2 at

545 day 0 (E), day 28 (F) and day 56 (G), (H) colonic histological score, (I) final body weight (J) fat

546 pad weight and (K) relative abundance of AIEC LF82 bacteria at day 56. Data are the means +/-

547 S.E.M ($N=3$). * $P < .05$ compared to water-treated group, determined by a one-way analysis of

548 variance corrected for multiple comparisons with a Bonferroni post-test.

549 **STAR METHODS**550 **KEY RESSOURCE TABLE AVAILABILITY**

REAGENT or RESOURCE	SOURCE	IDENTIFIER
Antibodies		
Anti-Mucin 2	Santa Cruz Biotechnology	Cat. # sc-15334; RRID: AB_2146667
Alexa Fluor 488 Goat Anti-Rabbit IgG	Invitrogen	Cat.# A11008; RRID: AB_143165
Chemicals, Peptides, and Recombinant Proteins		
Sodium carboxymethylcellulose	Sigma-Aldrich	419311
Polysorbate-80	Sigma-Aldrich	P1754
Phalloidin–Tetramethylrhodamine B isothiocyanate	Sigma-Aldrich	Cat.# P1951-.1MG
Rodent chow	LabDiet	Cat. # 5001
Luria Broth	BD	Cat. # BD 244620
Azoxymethane	Sigma-Aldrich	Cat. # A5486
Dextran sulfate sodium salt, colitis grade (36,000 - 50,000)	MP Biomedical	Cat. # SKU 02160110-CF
Critical Commercial Assays		
One-Step RT–PCR Kit with SYBR Green	Qiagen	Cat. # 204154
Duoset murine Lcn-2 ELISA kit	R&D Systems	Cat. # DY1857
In Situ Cell Death Detection Kit	Roche Diagnostics	Cat. # 11684795910
Deposited Data		
16S sequencing: unprocessed sequencing data	This paper	CRA003162
RNA-Seq: unprocessed sequencing data	This paper	CRA003155
Experimental Models: Organisms/Strains		
Mice: C57BL/6	Taconic Inc	Cat. # C57BL/6NTac
Mice: C57BL/6 IL10-/-	Taconic Inc	Cat. # GF-16006
Oligonucleotides		
See Table S1	This study	N/A
Software and Algorithms		
GraphPad Prism	GraphPad Software	Version 8

551

552

553

554

555 **RESOURCE AVAILABILITY**

556 **Lead Contact**

557 Further information and requests for resources and reagents should be directed to and will
558 be fulfilled by the Lead Contact, Benoit Chassaing (benoit.chassaing@inserm.fr).

559 **Materials Availability**

560 This study did not generate new unique reagents

561 **Data and Code Availability**

562 Unprocessed sequencing data are deposited in the Genome Sequence Archive (GSA) in
563 BIG Data Center , Beijing Institute of Genomics, Chinese Academy of Sciences, under accession
564 numbers CRA003155 and CRA003162, publicly accessible at <https://bigd.big.ac.cn/gsa>.

565

566 **EXPERIMENTAL MODEL AND SUBJECT DETAILS**

567 **Mice**

568 C57BL/6 mice (C57BL/6NTac) were maintained in gnotobiotic conditions in a germ-free
569 (GF) or Altered Schaedler flora state (ASF, containing the 8 bacteria *Clostridium sp.* (ASF356),
570 *Lactobacillus intestinalis* (ASF360), *Lactobacillus murinus* (ASF361), *Mucispirillum shaedleri*
571 (ASF457), *Eubacterium plexicaudatum* (ASF492), *Firmicutes bacterium* (ASF500), *Clostridium*
572 *sp.* (ASF502) and *Parabacteroides sp.* (ASF519)) in a Park Bioservices isolator as previously
573 described (Chassaing et al., 2015b). Germ-free C57BL/6 IL10^{-/-} male mice (C57BL/6NTac-
574 *Il10^{em8}Tac*; Taconic model GF-16006) were maintained in isolated ventilated cages Isocages
575 (Techniplast, West Chester, PA, USA) (Hecht et al., 2014). All mice were bred and housed at
576 Georgia State University (Atlanta, GA, USA) under institutionally-approved protocols (IACUC
577 # A17047 and A18006). Mice were fed autoclaved LabDiet rodent chow # 5021. ASF mice were

578 established by colonizing WT C57BL/6 GF mice with the complete Altered Schaedler flora (8
579 strains) using feces purchased from ASF Taconic Biosciences Inc. and resuspended in drinking
580 water, as previously described (Chassaing and Gewirtz, 2018). Mice used in this study were 4-5
581 weeks old.

582

583 **Materials**

584 Sodium carboxymethylcellulose (CMC, average MW ~250,000) and Polysorbate-80
585 (P80) were purchased from Sigma (Sigma, St. Louis, MO).

586

587 **METHOD DETAILS**

588 **Colonization with Adherent Invasive *Escherichia coli* strain LF82**

589 For mono-colonization of germ-free mice and colonization of ASF mice with Adherent
590 Invasive *Escherichia coli* (AIEC), reference strain LF82 and LF82- Δ *fliC* mutant were grown
591 overnight in 200 mL of LB at 37C without agitation. Bacterial suspensions with an OD_{620nm} of
592 2.0 were placed in the water bottles of germ-free or ASF C57Bl/6 mice placed in isolated
593 ventilated caging system (Isocage) that prevents exogenous bacterial contamination. One week
594 later, water solution was put back and supplemented with CMC or P80 (1.0%) (**Figure S1**). After
595 12 weeks, mice were euthanized and their organs were collected for downstream analysis.

596

597 **Emulsifier agent treatment**

598 Mice were exposed to CMC or P80 diluted in the drinking water (1.0%). The same water
599 (reverse-osmosis treated Atlanta city water) was used for the water-treated (control) group.
600 Emulsifier solutions were autoclaved and changed every week. Fresh feces were collected every

601 other week for downstream analysis. After 3 months of emulsifier treatment, body weight was
602 measured and blood was collected by retrobulbar intraorbital capillary plexus. Hemolysis-free
603 serum was generated by centrifugation of blood using serum separator tubes (Becton Dickinson,
604 Franklin Lakes, NJ). Mice were then euthanized and adipose weight, spleen weight, caecum
605 weight, colon length, and colon weight were measure. Organs were collected for downstream
606 analysis.

607

608 **Fasting blood glucose measurement**

609 Mice were placed in a clean cage and fasted for 5h. Blood glucose concentration was then
610 determined using a Nova Max Plus Glucose Meter and expressed in mg/dL.

611

612 **Colitis-associated cancer model**

613 Colitis-associated cancer (CAC) was induced as previously described with some
614 modifications (Greten et al., 2004; Viennois et al., 2017). As schematized in **Figure S1**, after
615 mono-association with AIEC reference strain LF82 and 4 weeks of emulsifier administration,
616 mice were intraperitoneally injected with AOM (10 mg/kg body weight) (Sigma-Aldrich, St.
617 Louis, MO) diluted in PBS and maintained on autoclaved chow diet and water or emulsifier-
618 supplemented water for 5 days. Mice were then subjected to two cycles of DSS treatment (MP
619 Biomedicals, Solon, OH, USA), in which each cycle consisted of 2.5% DSS for 7 days followed
620 by a 14-day recovery period with regular water or emulsifier-supplemented water. After
621 treatment, mice were fasted for 5h at which time blood was collected by retrobulbar intraorbital
622 capillary plexus. Hemolysis-free serum was generated by centrifugation of blood using serum
623 separator tubes (Becton Dickinson, Franklin Lakes, NJ). After colitis-associated cancer protocol,

624 mice were euthanized, and colon length, colon weight, spleen weight and adipose weight were
625 measure. Organs and blood were collected for downstream analysis. Colonic tumors were
626 counted and surface measured using a dissecting microscope. The total area of tumors for each
627 colon was determined.

628

629 **Adhesion and invasion assay**

630 The bacterial adhesion assay was performed as described previously (Boudeau et al.,
631 1999). Briefly, Intestine-407 cells were seeded in 24-well tissue culture plates with 4×10^5 cells
632 per well. Monolayers were then infected at a multiplicity of infection of 10 bacteria per cell in 1
633 ml of the cell culture medium without antibiotics and with heat-inactivated fetal calf serum
634 (FCS, PAA), using bacteria grown at 37°C in LB with or without CMC or P80 at various
635 concentration (0.0625, 0.2500 and 1.0000) and subsequently washed twice in PBS in order to
636 avoid any direct effect of emulsifier on adhesion and invasion processes. After a 3 h incubation
637 period at 37°C, monolayers were washed three times in phosphate-buffered saline (PBS, pH 7.2).
638 Epithelial cells were then lysed with 1% Triton X-100 (Euromedex) in deionized water. Samples
639 were diluted and plated onto Muller-Hinton agar plates to determine the number of colony-
640 forming units (CFU) corresponding to the total number of cell-associated bacteria (adherent and
641 intracellular bacteria). In order to determine the number of intracellular bacteria, fresh cell
642 culture medium containing 100 mg.ml^{-1} gentamicin was added for 1h to kill extracellular
643 bacteria. Monolayers were then lysed with 1% Triton X-100, and bacteria were quantified as
644 described above.

645

646

647

648 **Motility assay**

649 Bacterial strains were grown overnight at 37°C without agitation in LB broth with CMC
650 or P80 at 1.0% concentration, and 2µl portions of the culture were inoculated into the center of
651 0.3% LB agar plates. The plates were then incubated at 37°C, and motility was assessed
652 quantitatively 15 hours post inoculation by examining the circular swimming motion formed by
653 the growing motile bacterial cells.

654

655 **AIEC transcriptomic analysis**

656 Cultures were grown at 37°C in LB with or without CMC or P80 at various concentration
657 (0.0625, 0.2500 and 1.0000). Total mRNAs were extracted from overnight-cultured bacteria and
658 treated with DNase (Roche Diagnostics) to remove any contaminating genomic DNA. After
659 purification, RNA concentration and integrity were determined using Epoch Microplate
660 Spectrophotometer (Bio-Tek, Winooski, VT, USA) and agarose gel electrophoresis, respectively.
661 rRNAs were removed using Ribo-Zero® rRNA Removal Kit (Illumina) and total mRNAs were
662 then prepared for sequencing using Illumina TruSeq RNA kit according to the manufacturer's
663 protocol. Briefly, rRNA-depleted RNAs were fragmented, and converted to cDNA. After end
664 repair and ligation of adapters, mRNA libraries were amplified by PCR and validated using
665 BioAnalyser, according to manufacturer's recommendations. The purified library was then
666 subjected to sequencing using an Illumina NextSeq500 (single end, 75bp) at the Cornell
667 University sequencing core (Ithaca, NY). Sequencing data obtained were analyzed by alignment
668 against LF82 genome (both chromosome and plasmid (Miquel et al., 2010)) using bowtie 2
669 software (Langmead and Salzberg, 2012), and gene expression were compared between

670 conditions using cufflinks (Trapnell et al., 2012). Data were visualized using principal coordinate
671 analysis of the Euclidean distance, volcano plot created using R software, heatmap representation
672 using Morpheus (Chassaing et al., 2017b). Unprocessed sequencing data are deposited in the
673 Genome Sequence Archive (GSA)⁴⁶ in BIG Data Center 47, Beijing Institute of Genomics,
674 Chinese Academy of Sciences, under accession number CRA003155, publicly accessible at
675 <https://bigd.big.ac.cn/gsa>.

676

677 **Quantification of fecal lipocalin-2 (Lcn-2) by ELISA**

678 For quantification of fecal Lcn-2 by ELISA, frozen fecal samples were reconstituted in
679 PBS containing 0.1% Tween 20 to a final concentration of 100 mg/mL and vortexed for 20 min
680 to get a homogenous fecal suspension (Chassaing et al., 2012). These samples were then
681 centrifuged for 10 min at 14 000 g and 4°C. Clear supernatants were collected and stored at
682 -20°C until analysis. Lcn-2 levels were estimated in the supernatants using DuoSet murine Lcn-2
683 ELISA kit (R&D Systems, Minneapolis, MN, USA) using the colorimetric peroxidase substrate
684 tetramethylbenzidine, and optical density (OD) was read at 450 nm (Versamax microplate
685 reader).

686

687 **Colonic RNAs extraction and q-RT-PCR analysis**

688 Distal colon was collected during euthanasia and placed in RNAlater. Total RNAs were
689 isolated from colonic tissues using TRIzol (Invitrogen, Carlsbad, CA) according to the
690 manufacturer's instructions and as previously described (Chassaing et al., 2012). Quantitative
691 RT-PCR were performed using the Qiagen kit QuantiFast® SYBR® Green RT-PCR in a CFX96
692 apparatus (Bio-Rad, Hercules, CA) with specific mouse oligonucleotides (**Table S1**). Gene

693 expression are presented as relative values using the $\Delta\Delta\text{Ct}$ approach with 36B4 housekeeping
694 gene.

695

696

697 **Ki67 immunohistochemistry**

698 Mouse proximal colon devoid of tumor were fixed in 10%-buffered formalin for 24 h at
699 room temperature and subsequently embedded in paraffin. Tissues were sectioned at 5- μm
700 thickness and deparaffinized. Sections were incubated in sodium citrate buffer and cooked in a
701 pressure cooker for 10 minutes for antigen retrieval. Sections were then blocked with 5% goat
702 serum in TBS followed by one-hour incubation with anti-Ki67 (1:100, Vector Laboratories,
703 Burlingame, CA) at 37° C. After washing with TBS, sections were treated with biotinylated
704 secondary antibodies for 30 minutes at 37°C, and color development was performed using the
705 Vectastain ABC kit (Vector Laboratories). Sections were then counterstained with hematoxylin,
706 dehydrated, and coverslipped. Ki67-positive cells were counted per crypt.

707

708 **Terminal deoxynucleotidyl transferase deoxyuridine triphosphate nick-end labeling** 709 **(TUNEL)**

710 To quantitate the number of apoptotic cells in colonic epithelial cells, mouse proximal
711 colon devoid of tumor were fixed in 10%-buffered formalin for 24 h at room temperature,
712 embedded in paraffin, sectioned at 5- μm thickness, deparaffinized and stained for apoptotic
713 nuclei according to the manufacturer's instructions using the In Situ Cell Death Detection Kit
714 (Roche Diagnostics, Indianapolis, IN). TUNEL-positive cells overlapping with DAPI nuclear
715 staining were counted per crypt.

716

717 **H&E Staining of Colonic Tissue and Histopathologic Analysis**

718 Mouse colons were fixed in 10% buffered formalin for 24 hours at room temperature and
719 then embedded in paraffin. Tissues were sectioned at 5- μ m thickness and stained with
720 hematoxylin & eosin (H&E) using standard protocols. Images were acquired using a Lamina
721 (Perkin Elmer) at the Hist'IM platform (INSERM U1016, Paris, France). Histological scoring
722 was blindly determined on each colon as previously described (Chassaing et al., 2012; Katakura
723 et al., 2005). Briefly, each colon was assigned four scores based on the degree of epithelial
724 damage and inflammatory infiltrate in the mucosa, submucosa and muscularis/serosa (Katakura
725 et al., 2005). Each of the four scores was multiplied by a coefficient 1 if the change was focal, 2
726 if it was patchy and 3 if it was diffuse (Chassaing et al., 2012) and the 4 individual scores per
727 colon were added.

728

729 **Immunostaining of mucins and localization of bacteria by FISH**

730 Mucus immunostaining was paired with fluorescent *in situ* hybridization (FISH), as
731 previously described (Johansson and Hansson, 2012), in order to analyze bacteria localization at
732 the surface of the intestinal mucosa (Chassaing et al., 2015b; Chassaing et al., 2014b). Briefly,
733 colonic tissues (proximal colon, 2nd cm from the cecum) containing fecal material were placed
734 in methanol-Carnoy's fixative solution (60% methanol, 30% chloroform, 10% glacial acetic
735 acid) for a minimum of 3 h at room temperature. Tissues were then washed in methanol 2 x 30
736 min, ethanol 2 x 15 min, ethanol/xylene (1:1) 15 min and xylene 2 x 15 min, followed by
737 embedding in Paraffin with a vertical orientation. Five μ m sections were performed and dewax
738 by preheating at 60°C for 10 min, followed by xylene 60°C for 10 min, xylene for 10 min and

739 99.5% ethanol for 10 minutes. Hybridization step was performed at 50°C overnight with
740 EUB338 probe (5'-GCTGCCTCCCGTAGGAGT-3', with a 5' labeling using Alexa 647) diluted
741 to a final concentration of 10 µg/mL in hybridization buffer (20 mM Tris-HCl, pH 7.4, 0.9 M
742 NaCl, 0.1% SDS, 20% formamide). After washing 10 min in wash buffer (20 mM Tris-HCl, pH
743 7.4, 0.9 M NaCl) and 3 x 10 min in PBS, PAP pen (Sigma-Aldrich) was used to mark around the
744 section and block solution (5% fetal bovine serum in PBS) was added for 30 min at 4°C. Mucin-
745 2 primary antibody (rabbit H-300, Santa Cruz Biotechnology, Dallas, TX, USA) was diluted
746 1:1500 in block solution and apply overnight at 4°C. After washing 3 x 10 min in PBS, block
747 solution containing anti-rabbit Alexa 488 secondary antibody diluted 1:1500, Phalloidin-
748 Tetramethylrhodamine B isothiocyanate (Sigma-Aldrich) at 1µg/mL and Hoechst 33258 (Sigma-
749 Aldrich) at 10µg/mL was applied to the section for 2h. After washing 3 x 10 min in PBS slides
750 were mounted using Prolong anti-fade mounting media (Life Technologies, Carlsbad, CA,
751 USA). Observations were performed with a Zeiss LSM 700 confocal microscope with software
752 Zen 2011 version 7.1. This software was used to determine the distance between bacteria and
753 epithelial cell monolayer, as well as the mucus thickness.

754

755 **Immunostaining of mucins and localization of AIEC bacteria**

756 Mucus immunostaining was performed as described above. Anti Mucin-2 (from rabbit,
757 Gene Tex, Irvine, CA, United States) anti *Escherichia coli* (from goat Biorad, Hercules, CA,
758 United States) primary antibodies were diluted 1:500 in block solution and apply overnight at
759 4°C. After washing 3 x 10 min in PBS, block solution containing anti-rabbit Alexa 488 and anti-
760 goat Alexa 647 secondary antibodies diluted 1:1500, Phalloidin-Tetramethylrhodamine B
761 isothiocyanate (Sigma-Aldrich) at 1µg/mL and Hoechst 33258 (Sigma-Aldrich) at 10µg/mL was

762 applied to the section for 2h. After washing 3 x 10 min in PBS slides were mounted using
763 Prolong anti-fade mounting media (Life Technologies, Carlsbad, CA, USA). Image acquisition
764 were performed at the IMAG'IC Platform (INSERM U1016, Paris, France) using a Spinning-
765 Disk IXplore (Olympus). Olyvia software (Olympus) was used to determine the distance
766 between bacteria and epithelial cell monolayer.

767 **Inner mucus microdissection**

768 Microdissection were performed on an Arcturus® Laser Capture Microdissection system,
769 as previously described (Chassaing and Gewirtz, 2019). Inner mucus layers were selected and
770 collected on CapSure™ Macro LCM Caps (Arcturus) using a combination of infrared (IR)
771 capture and ultraviolet (UV) laser cutting. The membrane covering caps were subsequently
772 carefully collected, placed in clean DNA-free 0.5mL tubes, and store in -80°C until DNA
773 extraction.

774

775 **DNA extraction and 16S rRNA gene amplification from laser capture** 776 **microdissected mucus**

777 As previously described (Chassaing and Gewirtz, 2019), Qiagen QIAamp DNA Micro
778 Kit were used to isolate DNA from laser-microdissected inner mucus. 30µL of buffer ATL and
779 20µL of proteinase K were added to the microdissected samples and incubated at 56°C
780 overnight. 50µL of buffer ATL and 100µL of buffer AL were added, sample were mixed by
781 vortexing, and 100µL of ethanol was added followed by a 5 min incubation at room temperature.
782 The sample was next transferred to a QIAamp MinElute column (without the membrane) and
783 centrifuge at 6,000 g for 1 min. The column was washed with 500µL of buffer AW1 and 500µL
784 of buffer AW2 and dried with a 3 min centrifugation at 20,000 g. 20µL of DNA free water

785 (Mobio) were then applied to the center of the column, incubated at room temperature for 10min,
786 followed by a final centrifugation at 20,000 g for 1min in order to collect eluted DNA.
787 Microbiota analysis was subsequently performed by 16S rRNA gene sequencing using Illumina
788 technology, as described above.

789

790 **Fecal flagellin and lipopolysaccharide load quantification**

791 Levels of fecal bioactive flagellin and lipopolysaccharide (LPS) were quantified as
792 previously described (Chassaing et al., 2014a) using human embryonic kidney (HEK)-Blue-
793 mTLR5 and HEK-BlueTLR4 cells, respectively (Invivogen, San Diego, CA, USA) (Chassaing
794 et al., 2014a). Fecal material was resuspended in PBS to a final concentration of 100 mg/mL and
795 homogenized for 10 s using a Mini-Beadbeater-24 without the addition of beads to avoid bacteria
796 disruption. Samples were then centrifuged at 8000 g for 2 min and the resulting supernatant was
797 serially diluted and applied on mammalian cells. Purified *E. coli* flagellin and LPS (Sigma-
798 Aldrich) were used for standard curve determination using HEK-Blue-mTLR5 and HEK-Blue-
799 mTLR4 cells, respectively. After 24 h of stimulation, the cell culture supernatant was applied to
800 QUANTI-Blue medium (Invivogen) and the alkaline phosphatase activity was measured at 620
801 nm after 30 min.

802

803 **Bacterial RNAs extraction and q-RT-PCR analysis**

804 Cultures were grown at 37°C in LB with or without CMC or P80 at various concentration
805 (0.015625, 0.031250, 0.062500, 0.125000, 0.250000, 0.500000 and 1.000000). Total mRNAs
806 were extracted from overnight-cultured bacteria and treated with DNase (Roche Diagnostics) to
807 remove any contaminating genomic DNA. Total RNAs were amplified by RT-PCR using

808 specific primers to 16S, *fliC*, *flhDC*, *fimA* and *lpfA* (**Table S1**) on a Biorad CFX96 apparatus
809 (BioRad) using iTaq™ Universal SYBR® Green One-Step Kit (BioRad) with 0.25 µg of total
810 RNA. Amplification of a single expected PCR product was confirmed by electrophoresis on a
811 2% agarose gel.

812

813 **Microbiota analysis by 16S rRNA gene sequencing using Illumina technology**

814 16S rRNA gene amplification and sequencing were done using the Illumina MiSeq
815 technology following the protocol of Earth Microbiome Project with their modifications to the
816 MOBIO PowerSoil DNA Isolation Kit procedure for extracting DNA
817 (www.earthmicrobiome.org/emp-standard-protocols) (Caporaso et al., 2012; Gilbert et al., 2010).
818 Bulk DNA was extracted from frozen feces using a PowerSoil-htp kit from MoBio Laboratories
819 (Carlsbad, CA, USA) with mechanical disruption (bead-beating). The 16S rRNA genes, region
820 V4, were PCR amplified from each sample using a composite forward primer and a reverse
821 primer containing a unique 12-base barcode, designed using the Golay error-correcting scheme,
822 which was used to tag PCR products from respective samples (Caporaso et al., 2012). We used
823 the forward primer 515F 5'-
824 *AATGATACGGCGACCACCGAGATCTACACGCTXXXXXXXXXXXXTATGGTAATTGTG*
825 *TGYCAGCMGCCGCGGTAA*-3': the italicized sequence is the 5' Illumina adapter, the 12 X
826 sequence is the golay barcode, the bold sequence is the primer pad, the italicized and bold
827 sequence is the primer linker and the underlined sequence is the conserved bacterial primer
828 515F. The reverse primer 806R used was 5'-
829 *CAAGCAGAAGACGGCATAACGAGATAGTCAGCCAGCC GGACTACNVGGGTWTCTAAT*-
830 3': the italicized sequence is the 3' reverse complement sequence of Illumina adapter, the bold

831 sequence is the primer pad, the italicized and bold sequence is the primer linker and the
832 underlined sequence is the conserved bacterial primer 806R. PCR reactions consisted of Hot
833 Master PCR mix (Quantabio, Beverly, MA, USA), 0.2 μ M of each primer, 10-100 ng template,
834 and reaction conditions were 3 min at 95°C, followed by 30 cycles of 45 s at 95°C, 60s at 50°C
835 and 90 s at 72°C on a Biorad thermocycler. PCRs products were purified with Ampure magnetic
836 purification beads (Agencourt, Brea, CA, USA), and visualized by gel electrophoresis. Products
837 were then quantified (BIOTEK Fluorescence Spectrophotometer) using Quant-iT PicoGreen
838 dsDNA assay. A master DNA pool was generated from the purified products in equimolar ratios.
839 The pooled products were quantified using Quant-iT PicoGreen dsDNA assay and then
840 sequenced using an Illumina MiSeq sequencer (paired-end reads, 2 x 250 bp) at Cornell
841 University, Ithaca.

842

843 **16S rRNA gene sequence analysis**

844 Forward and reverse Illumina reads were joined using the fastq-join method (Aronesty,
845 2011, 2013), sequences were demultiplexed, quality filtered using Quantitative Insights Into
846 Microbial Ecology (QIIME, version 1.8.0) software package (Caporaso et al., 2010). QIIME
847 default parameters were used for quality filtering (reads truncated at first low-quality base and
848 excluded if: (1) there were more than three consecutive low quality base calls (2), less than 75%
849 of read length was consecutive high quality base calls (3), at least one uncalled base was present
850 (4), more than 1.5 errors were present in the bar code (5), any Phred qualities were below 20, or
851 (6) the length was less than 75 bases). Sequences were assigned to operational taxonomic units
852 (OTUs) using UCLUST algorithm (Edgar, 2010) with a 97% threshold of pairwise identity (with
853 the creation of new clusters with sequences that do not match the reference sequences), and

854 classified taxonomically using the Greengenes reference database 13_8 (McDonald et al., 2012).
855 A single representative sequence for each OTU was aligned and a phylogenetic tree was built
856 using FastTree (Price et al., 2009). The phylogenetic tree was used for computing the
857 unweighted UniFrac distances between samples (Lozupone et al., 2006; Lozupone and Knight,
858 2005), rarefaction were performed and used to compare abundances of OTUs across samples.
859 Principal coordinates analysis (PCoA) plots were used to assess the variation between
860 experimental group (beta diversity). Unprocessed sequencing data are deposited in the Genome
861 Sequence Archive (GSA)46 in BIG Data Center 47, Beijing Institute of Genomics, Chinese
862 Academy of Sciences, under accession number CRA003162, publicly accessible at
863 <https://bigd.big.ac.cn/gsa>.

864

865 **Bacterial density quantification by 16S rRNA qPCR**

866 Extracted DNAs were diluted 1/10 with sterile DNA-free water and amplified by quantitative
867 PCR using the 16S V4 specific primers 515F 5'-GTGYCAGCMGCCGCGGTAA-3' and 806R
868 5'-GGACTACNVGGGTWTCTAAT-3' or using the using the AIEC LF82 PTM specific
869 primers PTM-F 5'- CCATTCATGCAGCAGCTCTTT -3' and PTM-R 5'-
870 ATCGGACAACATTAGCGGTGT -3' on a LightCycler 480 (Roche) using QuantiFast SYBR®
871 Green PCR Kit (Qiagen). Amplification of a single expected PCR product was confirmed by
872 electrophoresis on a 2% agarose gel, and data are expressed as relative values normalized with
873 feces weight used for DNA extraction.

874

875 **QUANTIFICATION AND STATISTICAL ANALYSIS**

876 Results were expressed as mean \pm SEM. Significance was determined using one-way

877 group ANOVA with Bonferroni's multiple comparisons test (GraphPad Prism software, version
878 6.01). Differences were noted as significant $*p \leq 0.05$. For clustering analysis on principal
879 coordinate plots, categories were compared and statistical significance of clustering was
880 determined *via* Permanova.

881 **REFERENCES**

- 882 Aronesty, E. (2011). Command-line tools for processing biological sequencing data.
883 <http://code.google.com/p/ea-utils>.
- 884 Aronesty, E. (2013). Comparison of Sequencing Utility Programs. *The Open Bioinformatics*
885 *Journal* 7, 1-8.
- 886 Arthur, J.C., Perez-Chanona, E., Muhlbauer, M., Tomkovich, S., Uronis, J.M., Fan, T.J.,
887 Campbell, B.J., Abujamel, T., Dogan, B., Rogers, A.B., *et al.* (2012). Intestinal inflammation
888 targets cancer-inducing activity of the microbiota. *Science* 338, 120-123.
- 889 Barnich, N., Bringer, M.A., Claret, L., and Darfeuille-Michaud, A. (2004). Involvement of
890 lipoprotein NlpI in the virulence of adherent invasive *Escherichia coli* strain LF82 isolated from
891 a patient with Crohn's disease. *Infection and immunity* 72, 2484-2493.
- 892 Barnich, N., Carvalho, F.A., Glasser, A.L., Darcha, C., Jantscheff, P., Allez, M., Peeters, H.,
893 Bommelaer, G., Desreumaux, P., Colombel, J.F., *et al.* (2007). CEACAM6 acts as a receptor for
894 adherent-invasive *E. coli*, supporting ileal mucosa colonization in Crohn disease. *The Journal of*
895 *clinical investigation* 117, 1566-1574.
- 896 Boudeau, J., Glasser, A.L., Masseret, E., Joly, B., and Darfeuille-Michaud, A. (1999). Invasive
897 ability of an *Escherichia coli* strain isolated from the ileal mucosa of a patient with Crohn's
898 disease. *Infection and immunity* 67, 4499-4509.
- 899 Bretin, A., Lucas, C., Larabi, A., Dalmaso, G., Billard, E., Barnich, N., Bonnet, R., and Nguyen,
900 H.T.T. (2018). AIEC infection triggers modification of gut microbiota composition in genetically
901 predisposed mice, contributing to intestinal inflammation. *Sci Rep* 8, 12301.

902 Cani, P.D., Osto, M., Geurts, L., and Everard, A. (2012). Involvement of gut microbiota in the
903 development of low-grade inflammation and type 2 diabetes associated with obesity. *Gut*
904 *Microbes* 3, 279-288.

905 Caporaso, J.G., Kuczynski, J., Stombaugh, J., Bittinger, K., Bushman, F.D., Costello, E.K.,
906 Fierer, N., Pena, A.G., Goodrich, J.K., Gordon, J.I., *et al.* (2010). QIIME allows analysis of high-
907 throughput community sequencing data. *Nat Med* 7, 335-336.

908 Caporaso, J.G., Lauber, C.L., Walters, W.A., Berg-Lyons, D., Huntley, J., Fierer, N., Owens,
909 S.M., Betley, J., Fraser, L., Bauer, M., *et al.* (2012). Ultra-high-throughput microbial community
910 analysis on the Illumina HiSeq and MiSeq platforms. *The ISME journal* 6, 1621-1624.

911 Carvalho, F.A., Koren, O., Goodrich, J.K., Johansson, M.E., Nalbantoglu, I., Aitken, J.D., Su,
912 Y., Chassaing, B., Walters, W.A., Gonzalez, A., *et al.* (2012). Transient inability to manage
913 proteobacteria promotes chronic gut inflammation in TLR5-deficient mice. *Cell Host Microbe*
914 *12*, 139-152.

915 Chassaing, B., and Darfeuille-Michaud, A. (2011). The commensal microbiota and
916 enteropathogens in the pathogenesis of inflammatory bowel diseases. *Gastroenterology* *140*,
917 1720-1728.

918 Chassaing, B., and Darfeuille-Michaud, A. (2013). The sigmaE pathway is involved in biofilm
919 formation by Crohn's disease-associated adherent-invasive *Escherichia coli*. *J Bacteriol* *195*, 76-
920 84.

921 Chassaing, B., Etienne-Mesmin, L., Bonnet, R., and Darfeuille-Michaud, A. (2013). Bile salts
922 induce long polar fimbriae expression favouring Crohn's disease-associated adherent-invasive
923 *Escherichia coli* interaction with Peyer's patches. *Environ Microbiol* *15*, 355-371.

924 Chassaing, B., Garenaux, E., Carriere, J., Rolhion, N., Guerardel, Y., Barnich, N., Bonnet, R.,
925 and Darfeuille-Michaud, A. (2015a). Analysis of sigmaE regulon in Crohn disease-associated *E.*
926 *coli* revealed waaWVL operon involved in biofilm formation. *J Bacteriol.*

927 Chassaing, B., and Gewirtz, A.T. (2014). Gut microbiota, low-grade inflammation, and
928 metabolic syndrome. *Toxicol Pathol* 42, 49-53.

929 Chassaing, B., and Gewirtz, A.T. (2016). Has provoking microbiota aggression driven the
930 obesity epidemic? *Bioessays* 38, 122-128.

931 Chassaing, B., and Gewirtz, A.T. (2018). Mice harboring pathobiont-free microbiota do not
932 develop intestinal inflammation that normally results from an innate immune deficiency. *PLoS*
933 *One* 13, e0195310.

934 Chassaing, B., and Gewirtz, A.T. (2019). Identification of Inner Mucus-Associated Bacteria by
935 Laser Capture Microdissection. *Cell Mol Gastroenterol Hepatol* 7, 157-160.

936 Chassaing, B., Koren, O., Carvalho, F.A., Ley, R.E., and Gewirtz, A.T. (2014a). AIEC
937 pathobiont instigates chronic colitis in susceptible hosts by altering microbiota composition. *Gut*
938 63, 1069-1080.

939 Chassaing, B., Koren, O., Goodrich, J.K., Poole, A.C., Srinivasan, S., Ley, R.E., and Gewirtz,
940 A.T. (2015b). Dietary emulsifiers impact the mouse gut microbiota promoting colitis and
941 metabolic syndrome. *Nature* 519, 92-96.

942 Chassaing, B., Ley, R.E., and Gewirtz, A.T. (2014b). Intestinal epithelial cell toll-like receptor 5
943 regulates the intestinal microbiota to prevent low-grade inflammation and metabolic syndrome in
944 mice. *Gastroenterology* 147, 1363-1377 e1317.

945 Chassaing, B., Miles-Brown, J., Pellizzon, M., Ulman, E., Ricci, M., Zhang, L., Patterson, A.D.,
946 Vijay-Kumar, M., and Gewirtz, A.T. (2015c). Lack of soluble fiber drives diet-induced adiposity
947 in mice. *Am J Physiol Gastrointest Liver Physiol* 309, G528-541.

948 Chassaing, B., Raja, S.M., Lewis, J.D., Srinivasan, S., and Gewirtz, A.T. (2017a). Colonic
949 Microbiota Encroachment Correlates With Dysglycemia in Humans. *Cell Mol Gastroenterol*
950 *Hepatol* 4, 205-221.

951 Chassaing, B., Rolhion, N., de Vallee, A., Salim, S.Y., Prorok-Hamon, M., Neut, C., Campbell,
952 B.J., Soderholm, J.D., Hugot, J.P., Colombel, J.F., *et al.* (2011a). Crohn disease--associated
953 adherent-invasive *E. coli* bacteria target mouse and human Peyer's patches via long polar
954 fimbriae. *J Clin Invest* 121, 966-975.

955 Chassaing, B., Rolhion, N., Vallee, A., Salim, S.Y., Prorok-Hamon, M., Neut, C., Campbell,
956 B.J., Soderholm, J.D., Hugot, J.P., Colombel, J.F., *et al.* (2011b). Crohn disease-associated
957 adherent-invasive *E. coli* bacteria target mouse and human Peyer's patches via long polar
958 fimbriae. *J Clin Invest* 121, 966-975.

959 Chassaing, B., Srinivasan, G., Delgado, M.A., Young, A.N., Gewirtz, A.T., and Vijay-Kumar,
960 M. (2012). Fecal lipocalin 2, a sensitive and broadly dynamic non-invasive biomarker for
961 intestinal inflammation. *PLoS One* 7, e44328.

962 Chassaing, B., Van de Wiele, T., De Bodt, J., Marzorati, M., and Gewirtz, A.T. (2017b). Dietary
963 emulsifiers directly alter human microbiota composition and gene expression *ex vivo*
964 potentiating intestinal inflammation. *Gut* 66, 1414-1427.

965 Cox, S., Sandall, A., Smith, L., Rossi, M., and Whelan, K. (2020). Food additive emulsifiers: a
966 review of their role in foods, legislation and classifications, presence in food supply, dietary
967 exposure, and safety assessment. *Nutr Rev.*

968 Darfeuille-Michaud, A., Boudeau, J., Bulois, P., Neut, C., Glasser, A.L., Barnich, N., Bringer,
969 M.A., Swidsinski, A., Beaugerie, L., and Colombel, J.F. (2004). High prevalence of adherent-
970 invasive *Escherichia coli* associated with ileal mucosa in Crohn's disease. *Gastroenterology* *127*,
971 412-421.

972 Duprey, A., Reverchon, S., and Nasser, W. (2014). Bacterial virulence and Fis: adapting
973 regulatory networks to the host environment. *Trends Microbiol* *22*, 92-99.

974 Edgar, R.C. (2010). Search and clustering orders of magnitude faster than BLAST.
975 *Bioinformatics* *26*, 2460-2461.

976 EFSA (2015). Scientific Opinion on the re-evaluation of polyoxyethylene sorbitan monolaurate
977 (E 432), polyoxyethylene sorbitan monooleate (E 433), polyoxyethylene sorbitan monopalmitate
978 (E 434), polyoxyethylene sorbitan monostearate (E 435) and polyoxyethylene sorbitan tristearate
979 (E 436) as food additives. *EFSA Journal* *13*, 1-74.

980 EFSA (2017). Re-evaluation of celluloses E 460(i), E 460(ii), E 461, E 462, E 463, E 464, E 465,
981 E 466, E 468 and E 469 as food additives. *EFSA Journal* *16*, 1-104.

982 Fang, F.C., Frawley, E.R., Tapscott, T., and Vazquez-Torres, A. (2016). Bacterial Stress
983 Responses during Host Infection. *Cell Host Microbe* *20*, 133-143.

984 Franchi, L., Amer, A., Body-Malapel, M., Kanneganti, T.D., Ozoren, N., Jagirdar, R., Inohara,
985 N., Vandenabeele, P., Bertin, J., Coyle, A., *et al.* (2006). Cytosolic flagellin requires Ipaf for
986 activation of caspase-1 and interleukin 1beta in salmonella-infected macrophages. *Nat Immunol*
987 *7*, 576-582.

988 Gilbert, J.A., Meyer, F., Jansson, J., Gordon, J., Pace, N., Tiedje, J., Ley, R., Fierer, N., Field, D.,
989 Kyrpides, N., *et al.* (2010). The Earth Microbiome Project: Meeting report of the "1 EMP

990 meeting on sample selection and acquisition" at Argonne National Laboratory October 6 2010.
991 *Stand Genomic Sci* 3, 249-253.

992 Glasser, A.L., Boudeau, J., Barnich, N., Perruchot, M.H., Colombel, J.F., and Darfeuille-
993 Michaud, A. (2001). Adherent invasive *Escherichia coli* strains from patients with Crohn's
994 disease survive and replicate within macrophages without inducing host cell death. *Infection and*
995 *immunity* 69, 5529-5537.

996 Gomes-Neto, J.C., Mantz, S., Held, K., Sinha, R., Segura Munoz, R.R., Schmaltz, R., Benson,
997 A.K., Walter, J., and Ramer-Tait, A.E. (2017). A real-time PCR assay for accurate quantification
998 of the individual members of the Altered Schaedler Flora microbiota in gnotobiotic mice. *J*
999 *Microbiol Methods* 135, 52-62.

1000 Greten, F.R., Eckmann, L., Greten, T.F., Park, J.M., Li, Z.W., Egan, L.J., Kagnoff, M.F., and
1001 Karin, M. (2004). IKKbeta links inflammation and tumorigenesis in a mouse model of colitis-
1002 associated cancer. *Cell* 118, 285-296.

1003 Hayashi, F., Smith, K.D., Ozinsky, A., Hawn, T.R., Yi, E.C., Goodlett, D.R., Eng, J.K., Akira,
1004 S., Underhill, D.M., and Aderem, A. (2001). The innate immune response to bacterial flagellin is
1005 mediated by Toll-like receptor 5. *Nature* 410, 1099-1103.

1006 Johansson, M.E., and Hansson, G.C. (2012). Preservation of mucus in histological sections,
1007 immunostaining of mucins in fixed tissue, and localization of bacteria with FISH. *Methods Mol*
1008 *Biol* 842, 229-235.

1009 Jubelin, G., Desvaux, M., Schuller, S., Etienne-Mesmin, L., Muniesa, M., and Blanquet-Diot, S.
1010 (2018). Modulation of Enterohaemorrhagic *Escherichia coli* Survival and Virulence in the
1011 Human Gastrointestinal Tract. *Microorganisms* 6.

1012 Katakura, K., Lee, J., Rachmilewitz, D., Li, G., Eckmann, L., and Raz, E. (2005). Toll-like
1013 receptor 9-induced type I IFN protects mice from experimental colitis. *J Clin Invest* *115*, 695-
1014 702.

1015 Keyamura, K., Fujikawa, N., Ishida, T., Ozaki, S., Su'etsugu, M., Fujimitsu, K., Kagawa, W.,
1016 Yokoyama, S., Kurumizaka, H., and Katayama, T. (2007). The interaction of DiaA and DnaA
1017 regulates the replication cycle in *E. coli* by directly promoting ATP DnaA-specific initiation
1018 complexes. *Genes Dev* *21*, 2083-2099.

1019 Kuhn, R., Lohler, J., Rennick, D., Rajewsky, K., and Muller, W. (1993). Interleukin-10-deficient
1020 mice develop chronic enterocolitis. *Cell* *75*, 263-274.

1021 Langmead, B., and Salzberg, S.L. (2012). Fast gapped-read alignment with Bowtie 2. *Nat*
1022 *Methods* *9*, 357-359.

1023 Laudisi, F., Di Fusco, D., Dinallo, V., Stolfi, C., Di Grazia, A., Marafini, I., Colantoni, A.,
1024 Ortenzi, A., Alteri, C., Guerrieri, F., *et al.* (2018). The food additive maltodextrin promotes
1025 endoplasmic reticulum stress-driven mucus depletion and exacerbates intestinal inflammation.
1026 *Cell Mol Gastroenterol Hepatol*.

1027 Levine, A., Wine, E., Assa, A., Sigall Boneh, R., Shaoul, R., Kori, M., Cohen, S., Peleg, S.,
1028 Shamaly, H., On, A., *et al.* (2019). Crohn's Disease Exclusion Diet Plus Partial Enteral Nutrition
1029 Induces Sustained Remission in a Randomized Controlled Trial. *Gastroenterology* *157*, 440-450
1030 e448.

1031 Llewellyn, S.R., Britton, G.J., Contijoch, E.J., Vennaro, O.H., Mortha, A., Colombel, J.F.,
1032 Grinspan, A., Clemente, J.C., Merad, M., and Faith, J.J. (2018). Interactions Between Diet and
1033 the Intestinal Microbiota Alter Intestinal Permeability and Colitis Severity in Mice.
1034 *Gastroenterology* *154*, 1037-1046 e1032.

1035 Lozupone, C., Hamady, M., and Knight, R. (2006). UniFrac--an online tool for comparing
1036 microbial community diversity in a phylogenetic context. *BMC Bioinformatics* 7, 371.

1037 Lozupone, C., and Knight, R. (2005). UniFrac: a new phylogenetic method for comparing
1038 microbial communities. *Appl Environ Microbiol* 71, 8228-8235.

1039 McDonald, D., Price, M.N., Goodrich, J., Nawrocki, E.P., DeSantis, T.Z., Probst, A., Andersen,
1040 G.L., Knight, R., and Hugenholtz, P. (2012). An improved Greengenes taxonomy with explicit
1041 ranks for ecological and evolutionary analyses of bacteria and archaea. *ISME J* 6, 610-618.

1042 Miles, J.P., Zou, J., Kumar, M.V., Pellizzon, M., Ulman, E., Ricci, M., Gewirtz, A.T., and
1043 Chassaing, B. (2017). Supplementation of Low- and High-fat Diets with Fermentable Fiber
1044 Exacerbates Severity of DSS-induced Acute Colitis. *Inflamm Bowel Dis* 23, 1133-1143.

1045 Miquel, S., Peyretailade, E., Claret, L., de Vallee, A., Dossat, C., Vacherie, B., Zineb el, H.,
1046 Segurens, B., Barbe, V., Sauvanet, P., *et al.* (2010). Complete genome sequence of Crohn's
1047 disease-associated adherent-invasive *E. coli* strain LF82. *PLoS One* 5.

1048 Ng, S.C., Shi, H.Y., Hamidi, N., Underwood, F.E., Tang, W., Benchimol, E.I., Panaccione, R.,
1049 Ghosh, S., Wu, J.C.Y., Chan, F.K.L., *et al.* (2017). Worldwide incidence and prevalence of
1050 inflammatory bowel disease in the 21st century: a systematic review of population-based studies.
1051 *Lancet*.

1052 Nickerson, K.P., Homer, C.R., Kessler, S.P., Dixon, L.J., Kabi, A., Gordon, I.O., Johnson, E.E.,
1053 de la Motte, C.A., and McDonald, C. (2014). The dietary polysaccharide maltodextrin promotes
1054 *Salmonella* survival and mucosal colonization in mice. *PLoS One* 9, e101789.

1055 Nickerson, K.P., and McDonald, C. (2012). Crohn's disease-associated adherent-invasive
1056 *Escherichia coli* adhesion is enhanced by exposure to the ubiquitous dietary polysaccharide
1057 maltodextrin. *PLoS One* 7, e52132.

1058 Palmela, C., Chevarin, C., Xu, Z., Torres, J., Sevrin, G., Hirten, R., Barnich, N., Ng, S.C., and
1059 Colombel, J.F. (2018). Adherent-invasive *Escherichia coli* in inflammatory bowel disease. *Gut*
1060 *67*, 574-587.

1061 Price, M.N., Dehal, P.S., and Arkin, A.P. (2009). FastTree: computing large minimum evolution
1062 trees with profiles instead of a distance matrix. *Mol Biol Evol* *26*, 1641-1650.

1063 Roberts, C.L., Keita, A.V., Duncan, S.H., O'Kennedy, N., Soderholm, J.D., Rhodes, J.M., and
1064 Campbell, B.J. (2010). Translocation of Crohn's disease *Escherichia coli* across M-cells:
1065 contrasting effects of soluble plant fibres and emulsifiers. *Gut* *59*, 1331-1339.

1066 Roberts, C.L., Rushworth, S.L., Richman, E., and Rhodes, J.M. (2013). Hypothesis: Increased
1067 consumption of emulsifiers as an explanation for the rising incidence of Crohn's disease. *J*
1068 *Crohns Colitis* *7*, 338-341.

1069 Rodriguez-Palacios, A., Harding, A., Menghini, P., Himmelman, C., Retuerto, M., Nickerson,
1070 K.P., Lam, M., Croniger, C.M., McLean, M.H., Durum, S.K., *et al.* (2018). The Artificial
1071 Sweetener Splenda Promotes Gut Proteobacteria, Dysbiosis, and Myeloperoxidase Reactivity in
1072 Crohn's Disease-Like Ileitis. *Inflamm Bowel Dis* *24*, 1005-1020.

1073 Rolhion, N., Carvalho, F.A., and Darfeuille-Michaud, A. (2007). OmpC and the sigma(E)
1074 regulatory pathway are involved in adhesion and invasion of the Crohn's disease-associated
1075 *Escherichia coli* strain LF82. *Molecular microbiology* *63*, 1684-1700.

1076 Sabino, J., Lewis, J.D., and Colombel, J.F. (2019). Treating Inflammatory Bowel Disease With
1077 Diet: A Taste Test. *Gastroenterology* *157*, 295-297.

1078 Sellon, R.K., Tonkonogy, S., Schultz, M., Dieleman, L.A., Grenther, W., Balish, E., Rennick,
1079 D.M., and Sartor, R.B. (1998). Resident enteric bacteria are necessary for development of

1080 spontaneous colitis and immune system activation in interleukin-10-deficient mice. *Infect*
1081 *Immun* 66, 5224-5231.

1082 Sevrin, G., Massier, S., Chassaing, B., Agus, A., Delmas, J., Denizot, J., Billard, E., and Barnich,
1083 N. (2018). Adaptation of adherent-invasive *E. coli* to gut environment: impact on flagellum
1084 expression and bacterial colonization ability. *Gut Microbes* *in press*.

1085 Suez, J., Korem, T., Zeevi, D., Zilberman-Schapira, G., Thaiss, C.A., Maza, O., Israeli, D.,
1086 Zmora, N., Gilad, S., Weinberger, A., *et al.* (2014). Artificial sweeteners induce glucose
1087 intolerance by altering the gut microbiota. *Nature* 514, 181-186.

1088 Tobacman, J.K. (2001). Review of harmful gastrointestinal effects of carrageenan in animal
1089 experiments. *Environ Health Perspect* 109, 983-994.

1090 Trapnell, C., Roberts, A., Goff, L., Pertea, G., Kim, D., Kelley, D.R., Pimentel, H., Salzberg,
1091 S.L., Rinn, J.L., and Pachter, L. (2012). Differential gene and transcript expression analysis of
1092 RNA-seq experiments with TopHat and Cufflinks. *Nature protocols* 7, 562-578.

1093 Vazeille, E., Chassaing, B., Buisson, A., Dubois, A., de Vallee, A., Billard, E., Neut, C.,
1094 Bommelaer, G., Colombel, J.F., Barnich, N., *et al.* (2016). GipA Factor Supports Colonization of
1095 Peyer's Patches by Crohn's Disease-associated *Escherichia Coli*. *Inflamm Bowel Dis* 22, 68-81.

1096 Viennois, E., and Chassaing, B. (2018). First victim, later aggressor: How the intestinal
1097 microbiota drives the pro-inflammatory effects of dietary emulsifiers? *Gut Microbes*, 1-4.

1098 Viennois, E., Gewirtz, A.T., and Chassaing, B. (2019). Chronic Inflammatory Diseases: Are We
1099 Ready for Microbiota-based Dietary Intervention? *Cell Mol Gastroenterol Hepatol* 8, 61-71.

1100 Viennois, E., Merlin, D., Gewirtz, A.T., and Chassaing, B. (2017). Dietary Emulsifier-Induced
1101 Low-Grade Inflammation Promotes Colon Carcinogenesis. *Cancer Res* 77, 27-40.

1102 Vijay-Kumar, M., Aitken, J.D., Carvalho, F.A., Cullender, T.C., Mwangi, S., Srinivasan, S.,
1103 Sitaraman, S.V., Knight, R., Ley, R.E., and Gewirtz, A.T. (2010). Metabolic syndrome and
1104 altered gut microbiota in mice lacking Toll-like receptor 5. *Science* 328, 228-231.
1105 Xavier, R.J., and Podolsky, D.K. (2007). Unravelling the pathogenesis of inflammatory bowel
1106 disease. *Nature* 448, 427-434.
1107 Zeevi, D., Korem, T., Zmora, N., Israeli, D., Rothschild, D., Weinberger, A., Ben-Yacov, O.,
1108 Lador, D., Avnit-Sagi, T., Lotan-Pompan, M., *et al.* (2015). Personalized Nutrition by Prediction
1109 of Glycemic Responses. *Cell* 163, 1079-1094.
1110 Zmora, N., Suez, J., and Elinav, E. (2019). You are what you eat: diet, health and the gut
1111 microbiota. *Nat Rev Gastroenterol Hepatol* 16, 35-56.
1112

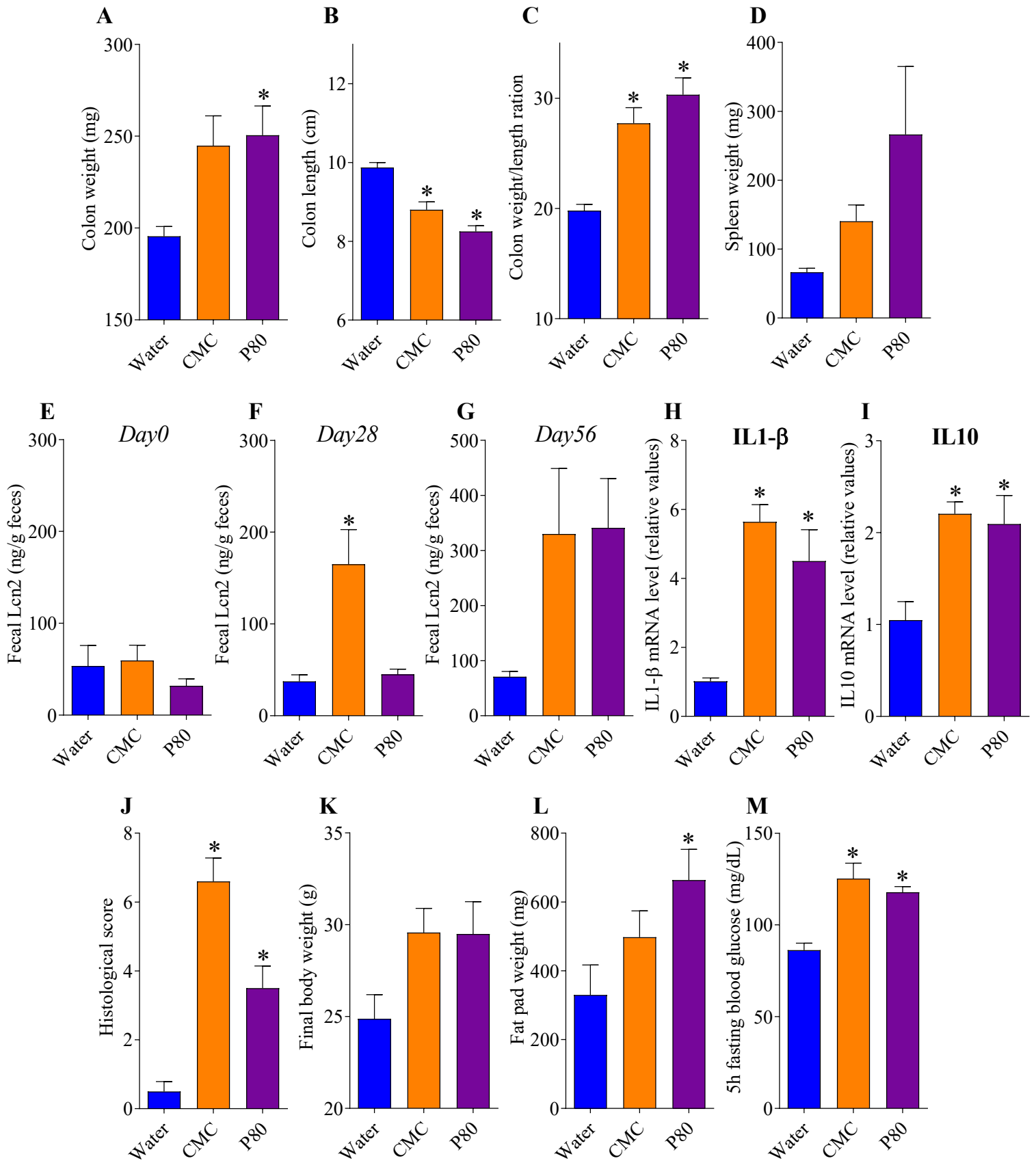


Figure 1: Colonization by adherent-invasive *Escherichia coli* bacteria is sufficient to promote detrimental effects of emulsifiers in normally protected ASF mice.

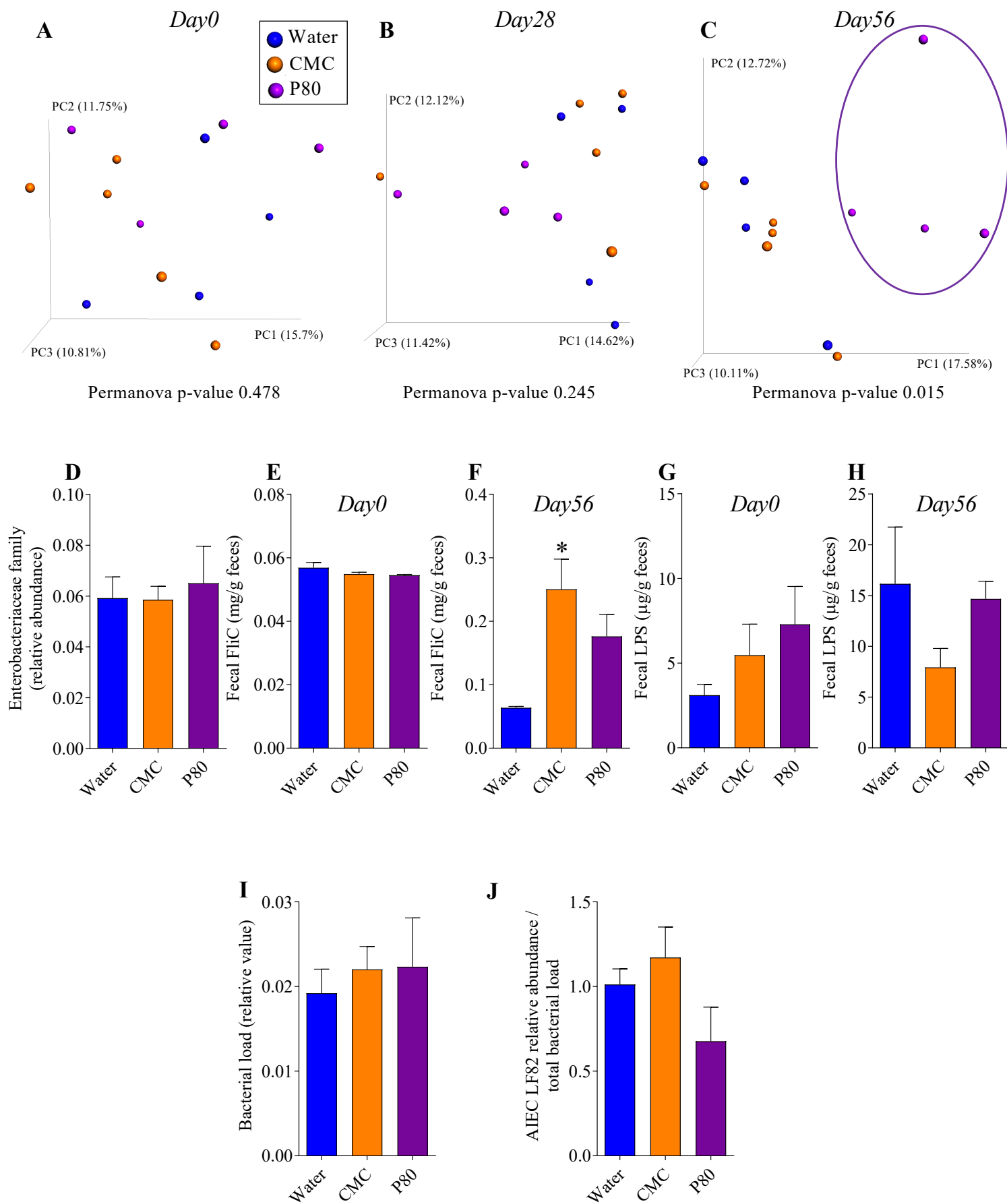


Figure 2: Colonization of ASF mice by adherent-invasive *Escherichia coli* bacteria is sufficient to induce emulsifier-mediated alterations in microbiota.

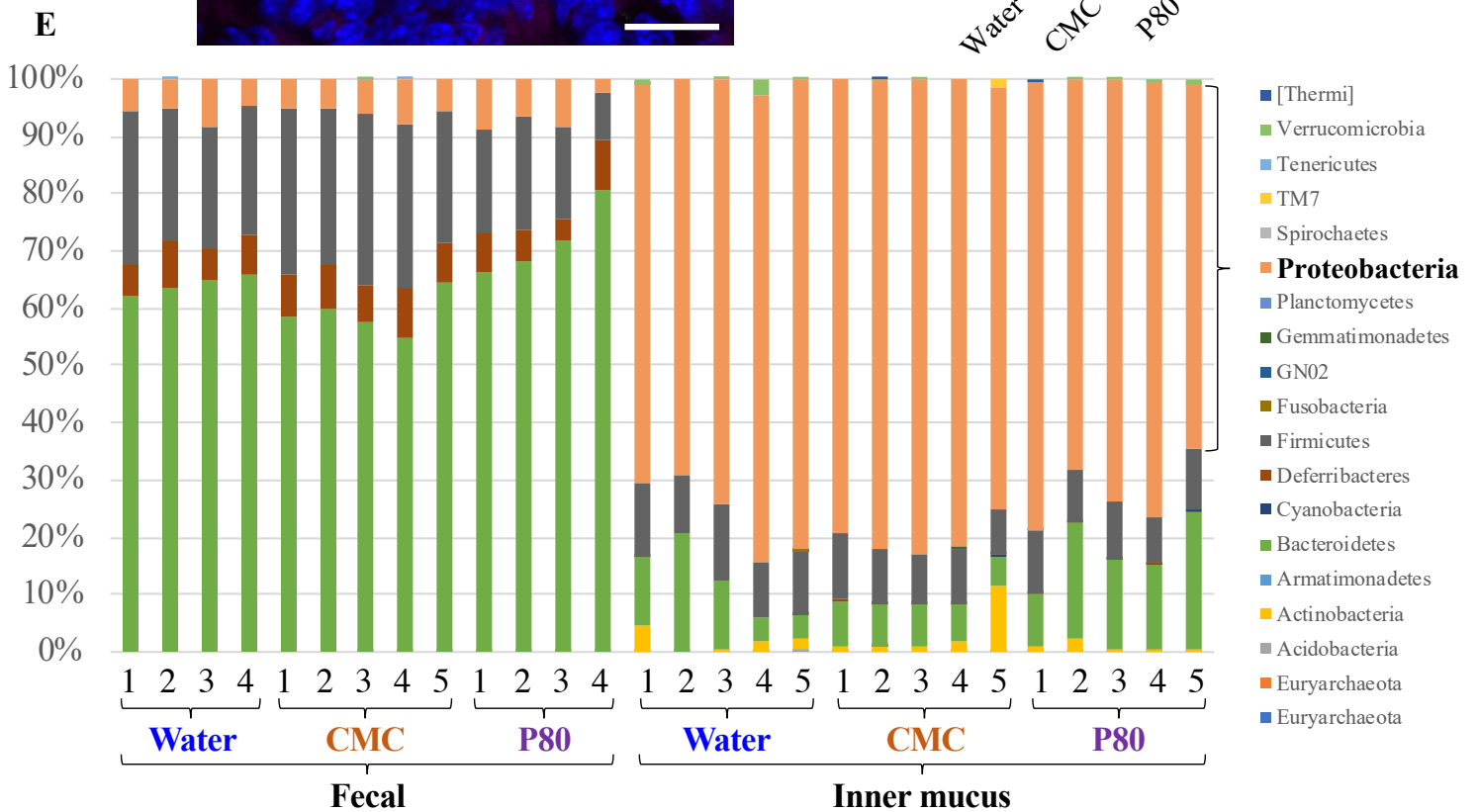
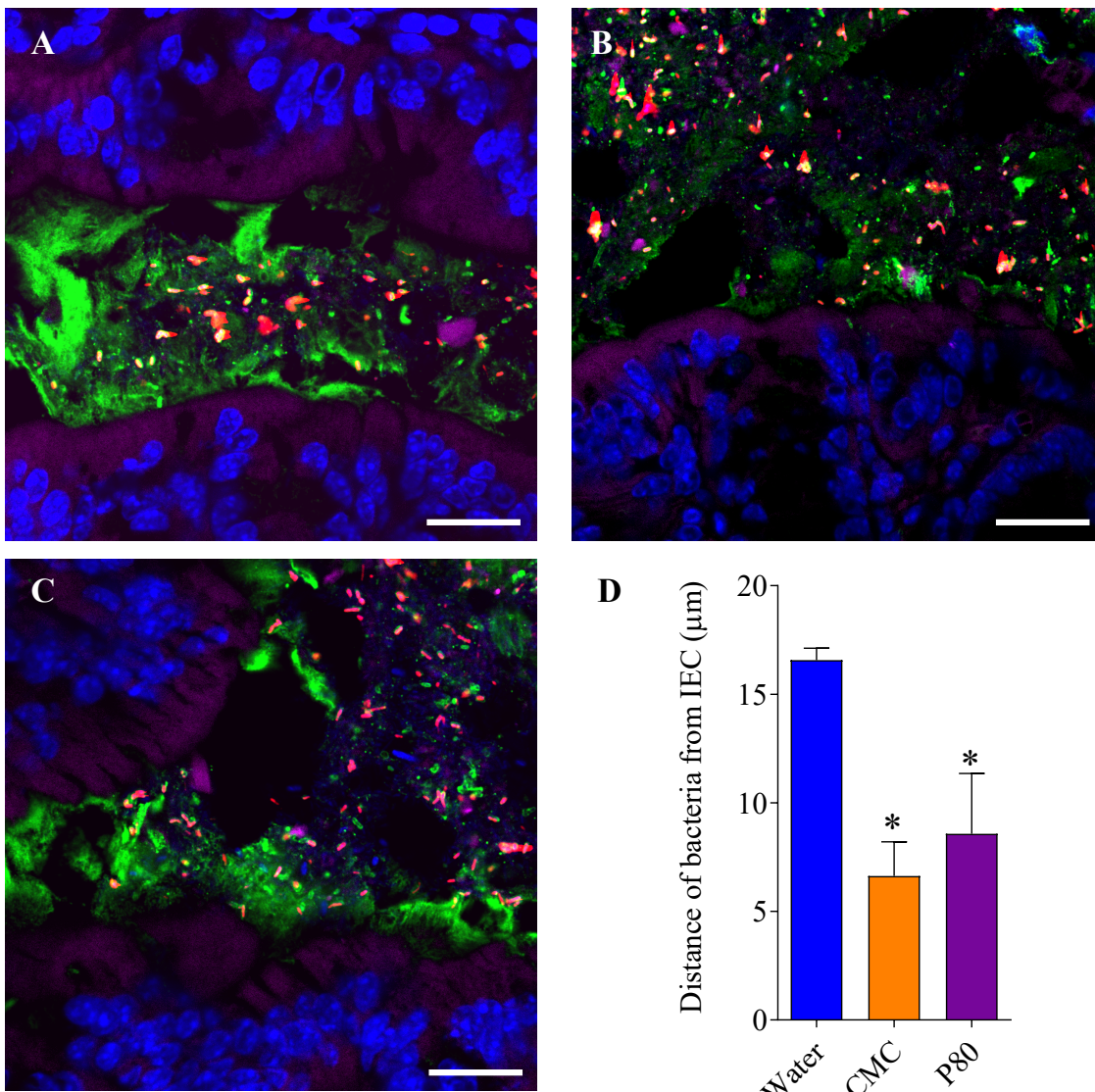


Figure 3: Colonization by adherent-invasive *Escherichia coli* bacteria is sufficient to induce microbiota encroachment in normally protected ASF mice.

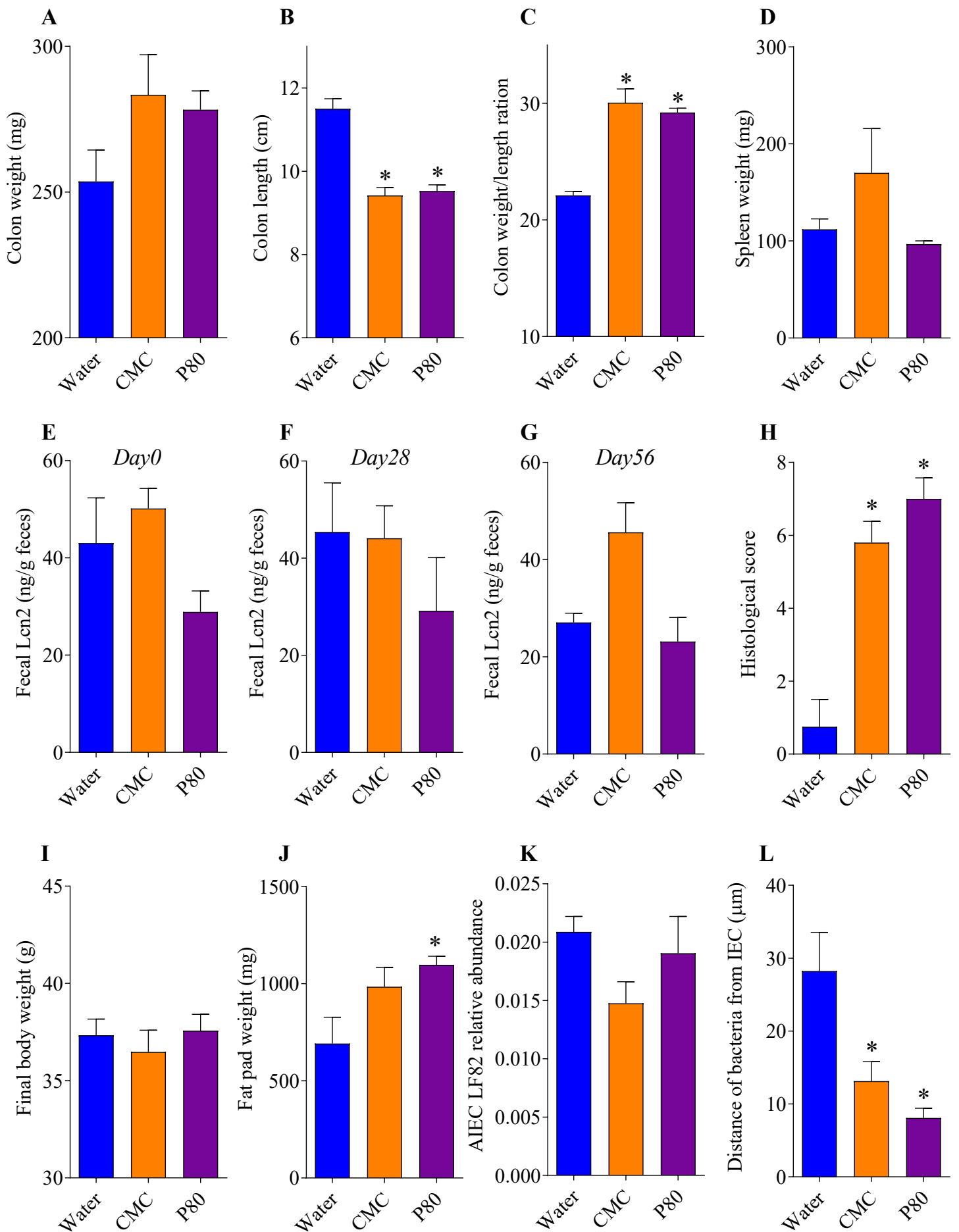


Figure 4: Mono-colonization by adherent-invasive *Escherichia coli* bacteria is sufficient to drive detrimental effects of emulsifiers in WT mice.

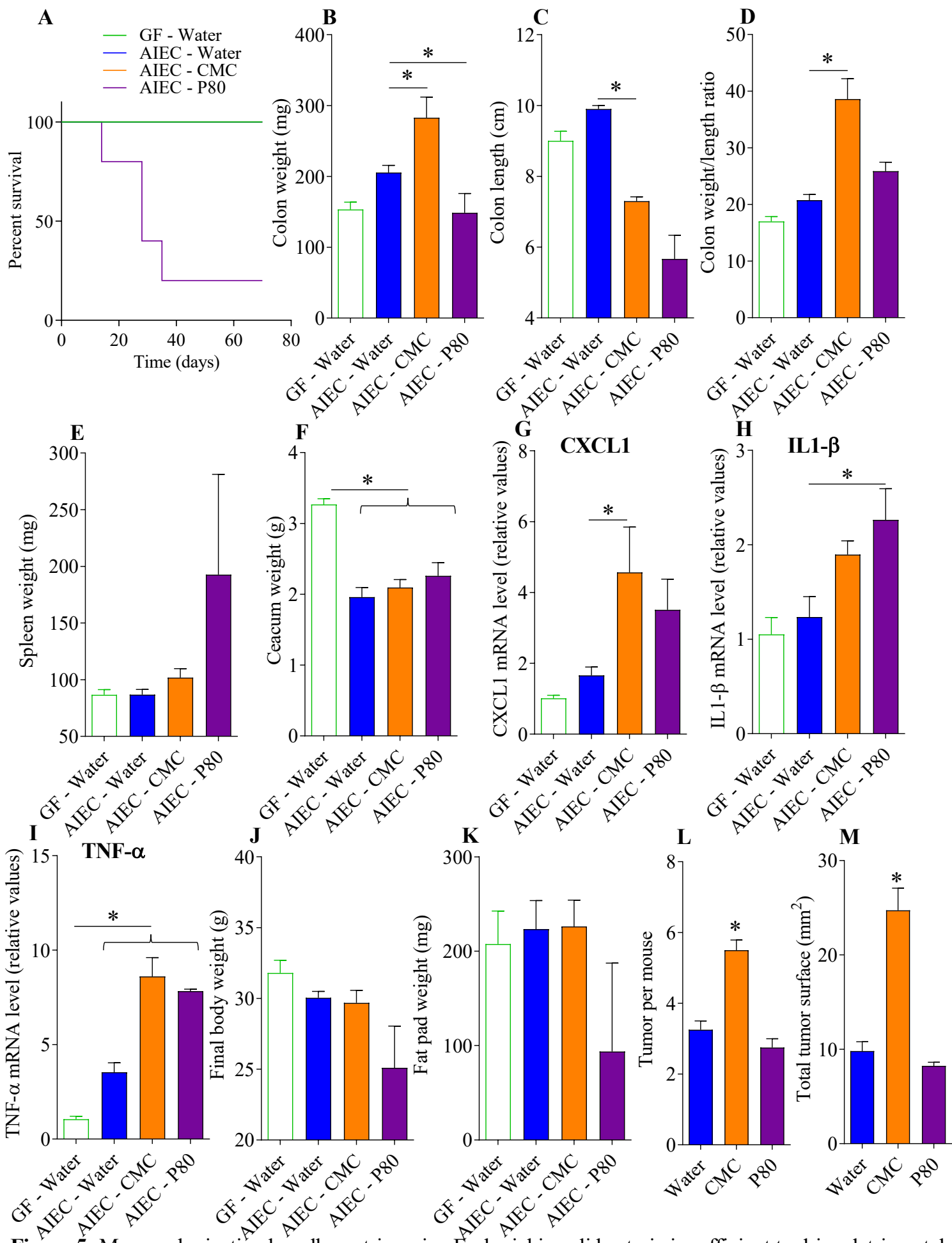


Figure 5: Mono-colonization by adherent-invasive *Escherichia coli* bacteria is sufficient to drive detrimental effects of emulsifiers in IL10^{-/-} mice and promotion of colon cancer in WT.

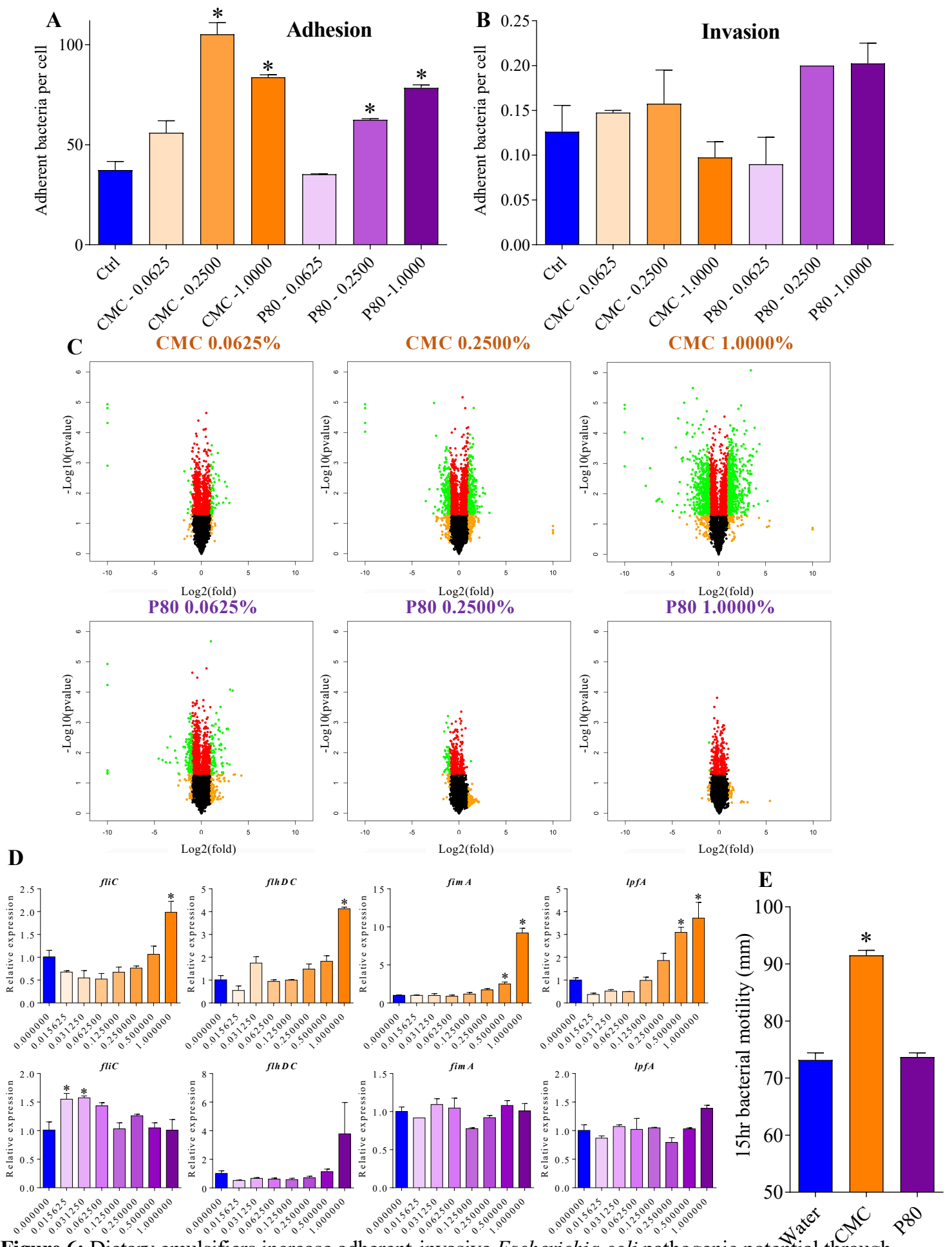


Figure 6: Dietary emulsifiers increase adherent-invasive *Escherichia coli* pathogenic potential through transcriptome modulation.

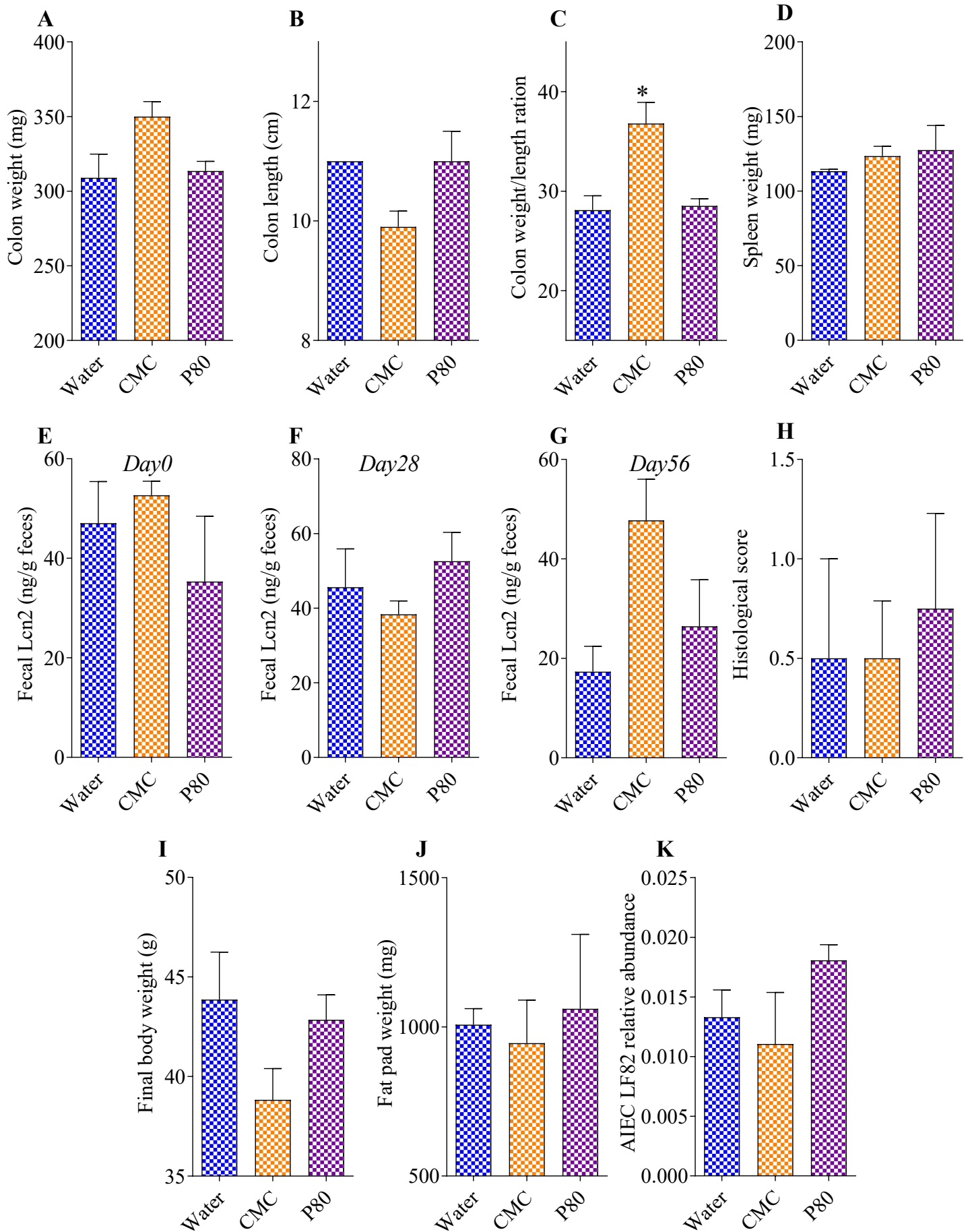


Figure 7: Bacterial flagellin contributes to AIEC-mediated emulsifier detrimental effects.

